CCI

BIOMASS

PRODUCT USER GUIDE

YEAR 3

VERSION 3.0

DOCUMENT REF:	CCI_BIOMASS_PUG_V3
DELIVERABLE REF:	D4.3_PUG
VERSION:	3.0
CREATION DATE:	2021-07-05
LAST MODIFIED	2021-07-05

Document Authorship

	NAME	FUNCTION	ORGANISATION	SIGNATURE	DATE
PREPARED	M. Santoro	WP6 Lead	GAMMA RS		
PREPARED					
PREPARED					
PREPARED					
PREPARED					
PREPARED					
PREPARED					
PREPARED					
VERIFIED	R. Lucas	Project Manager	Aberystwyth University		
VERIFIED	H. Kay	Project Coordinator	Aberystwyth University		
VERIFIED	S. Quegan	Science Leader	Sheffield University		
APPROVED					

Document Distribution

ORGANISATION	NAME	QUANTITY
ESA	Frank Seifert	

Document History

VERSION	DATE	DESCRIPTION	APPROVED
0.1	2019-09-01	First draft version	
1.0	2019-09-03	Finalised version of year 1 CCI BIOMASS data products	
2.0	2020-10-07	Finalised version of year 2 CCI BIOMASS data products	
3.0	2021-07-05	Finalised version of year 3 CCI BIOMASS data products	

Document Change Record (from Year 1 to Year 2)

VERSION	DATE	DESCRIPTION	APPROVED
2.0	2020-10-07	Updated the description of the year 1 data product (AGB map for the year 2017). Added the description of the year 2 data products (AGB maps for the years 2010 and 2018)	
3.0	2021-07-05	Updated the description of the year 2 data products (AGB maps for the epochs 2010, 2017 and 2018). Added the description of the year 3 data products (AGB change maps for 2010-2018 and 2017-2018).	

TABLE OF CONTENTS

LIST OF TABLES

LIST OF FIGURES

SYMBOLS AND ACRONYMS

AGB	Above Ground Biomass
ALOS	Advanced Land Observing Satellite
ATBD	Algorithm Theoretical Basis Document
BCEF	Biomass Expansion and Conversion Factor
BGB	Below-ground biomass
CCI	Climate Change Initiative
CF	Climate and Forecast
CMUG	Climate Modellers User Group
CRDP	Climate Research Data Package
DEM	Digital Elevation Model
DUE	Date User Element
E3UB	End-to-end Uncertainty Budget
ECV	Essential Climate Variable
EO	Earth Observation
ESA	European Space Agency
FAO	Food and Agriculture Organization
FBD	Fine Beam Dual-
FTP	File Transfer Protocol
GCOS	Global Carbon Observing System
GEDI	Global Ecosystem Dynamics Investigation
GSV	Growing stock volume
JAXA	Japan Aerospace Exploration Agency
NFI	National Forest Inventory
NISAR	NASA-ISRO Synthetic Aperture Radar
PALSAR	Phased Array-type L-band Synthetic Aperture Radar
PUG	Product User Guide
PVASR	Product Validation and Algorithm Selection Report
SAR	Synthetic Aperture Radar
SD	SD
UN-REDD	United Nations Reducing Emissions from Deforestation and Forest Degradation
URD	User Requirement Document
WB	Wide Beam
WGS	World Geodetic System

Table 1: Reference Documents

ID	Title	Issue	Date
RD-1	Climate Research Data Package	3.0	2021-07-02
RD-2	Users Requirements Document	2.0	2021-01-06
RD-3	Algorithm Theoretical Basis Document	3.0	2021-06-14
RD-4	End-to-End ECV Uncertainty Budget	3.0	2020-06-14
RD-5	Product Regional Assessment & Intercomparison Report	3.0	2020-12-17
RD-6	Product Validation & Intercomparison Report	3.0	2021-07-29

1. Introduction

1.1. Context

The aim of the Climate Change Initiative (CCI) Programme is to advance scientific understanding of the climate system and climate change by producing long-term datasets that meet climate data quality conditions (IPCC, 2003) and that can be readily linked to climate models. A basic input to this process is the series of reports by the Global Carbon Observing System (GCOS) that set out a continually reviewed set of Essential Climate Variables (ECVs) and a process to implement the acquisition of these ECVs. The primary motivation for listing above-ground biomass (AGB) as an ECV is that AGB is crucial in order to understand both the source and sink terms in the global carbon cycle (which is fundamentally what drives climate change by controlling the carbon dioxide in the atmosphere). The source term comes from carbon emissions when biomass is lost due to fire and land use change; the sink term arises because growing forests extract CO_2 from the atmosphere and tie it up in long-lasting wood and soil stores.

Although satellite data limitations are such that biomass products from space cannot provide the 30-year climate quality datasets sought by the climate community, the CCI BIOMASS project is a start in this direction since spaceborne data records exist and their usefulness to derive spatially explicit estimates of AGB have been demonstrated. In addition, the coming years will see a wealth of missions targeting biomass as one of the primary objectives. As such, this project sets out not only to produce the best possible validated maps of biomass suitable for climate modelling with existing data, but also ensures that biomass estimation methods being developed are sustainable to include new and additional data streams towards progressively more accurate biomass products.

1.2. Purpose of document

The Product User Guide (PUG) provides a description of the data products generated and disseminated by the CCI BIOMASS project as part of the Climate Research Data Package (CRDP) [RD-1]. The data products are here presented in terms of a brief summary of the algorithms used, their thematic content and technical specifications (data format, file names and metadata).

This PUG describes the data products obtained at the end of the third year of the CCI BIOMASS project and referred to as Version 3.0.

1.3. Contents

The document consists of the following sections:

Section 2 provides an overview of the CCI BIOMASS project;
Sections 3 and 4 describe the data products provided as part of the CRDP
Section 5 gives indication on how to use the CCI BIOMASS datasets
Section 6 provides details on data access and data policy.

Appendices include additional information on the datasets with the intention to act as reference guides for the interpretation of the AGB map and the map data format.

For correct use of the CCI BIOMASS datasets, it is strongly recommended to refer to Section 5.

Please contact the data producer (Maurizio Santoro, Gamma Remote Sensing, santoro@gamma-rs.ch) for questions related to the use of the AGB maps and the AGB change maps.

2. CCI Biomass Project

2.1. AGB and Earth Observation

According to the Food and Agriculture Organization (FAO), above-ground biomass is defined as the amount of living biomass (organic matter) stored in vegetation above the soil including stem, stump, branches, bark, seeds and foliage, expressed as dry weight. This is opposed to below-ground biomass (BGB) that refers to the amount of biomass stored in vegetation below the soil. AGB is sometimes differentiated between woody and non-woody vegetation. AGB stored in woody vegetation requires a definition of the minimum size of trees that count as woody vegetation. Non-woody vegetation consists of trees smaller than a given threshold on tree size, shrubs, and all other non-herbaceous live vegetation. For the definition adopted in this work, please refer to Section 3.1.

In this context, AGB is here referred to in terms of biomass density, i.e., the amount of living biomass per unit area. Accordingly, AGB is expressed in units of mass of dry matter per unit ground area, i.e., Mg ha^{-1} (Megagrams per hectare).

Precise estimates of AGB require destructive sampling. This is not viable when the aim is to quantify the overall biomass pool on Earth, so alternative methods that predict AGB from in situ measurements and model-based approaches come into play. Allometries derived from felled sample trees, i.e., equations linking various structural parameters of a tree to biomass, permit non-destructive sampling. Yet they require ground surveys, which can be costly, imply non-trivial logistics and are time consuming. To overcome some of these issues, terrestrial, airborne and spaceborne remote sensing techniques have been developed in recent years as an alternative or complement to local surveys. Accordingly, models relating the remote sensing observables to measurements collected in situ have been developed. A major advantage of airborne and spaceborne remote sensing as tools to estimate AGB is their ability to cover large areas at less cost than ground surveys. However, a map of AGB obtained from remote sensing observations is an estimate of the true biomass on the ground and relies heavily on the accuracy of the models used to convert measurements of the observables to AGB.

The remote sensing community has made continual efforts to generate wall-to-wall datasets of AGB that span a wide geographical region, a specific biome or the entire globe. The CCI Programme recognized the maturity of Earth Observations to provide global and repeated measurements of land surfaces and gave a significant boost to generation of global climate data records from space. The CCI Programme added the ECV AGB to its suite of CCI+ projects, with primary objective to generate climate-relevant time records of biomass estimates that fulfil requirements set by GCOS. Key to this is the integration of multiple Earth Observation data sources, local surveys and an inter-disciplinary team that includes remote sensing experts, ecologists, statisticians and climate modellers.

2.2. Users' requirements

The CCI BIOMASS project was built on the requirements set by GCOS in terms of spatial detail, temporal resolution and thematic accuracy of AGB datasets. The requirement is for AGB to be provided wall-to-wall over the entire globe for all major woody biomes, with spatial resolution between 500 m and 1 km (based on satellite observations of 100-200 m), and with a relative error of less than 20% where AGB exceeds 50 Mg/ha^{-1} and an error of 10 Mg/ha^{-1} where the AGB is below 50 Mg/ha^{-1}.

Furthermore, the AGB data products delivered by the CCI BIOMASS project need to take into account indications, requirements and wishes by potential users of such data products. These were reported in the User Requirement Document (URD) [RD-2] of the CCI BIOMASS project, which was compiled at the beginning of the project after the first CCI BIOMASS User Workshop (September 2018) and a Climate Modellers User Group (CMUG) meeting (October 2018). The URD includes input from climate and carbon modelling, ecology, geography, resource assessment, climate policy and other user families. Ultimately, the user requirements were found to cover the needs of two different communities: the modelling community and the policy community.

Table 2-1 summarizes the requirements reported in the URD. Requirements were divided into minimum and desired. Although these two communities agree on many of the major desirable properties of the products (text in bold), the requirements on spatial resolution are different (text in italic). The climate and carbon modelling community, which is the primary focus of CCI BIOMASS, requires unbiased AGB estimates but is more relaxed on the spatial resolution because of the coarse grid-cell size of climate models. The community concerned with United Nations Framework Convention on Climate Change (UNFCCC) reporting and the UN Reducing Emissions from Deforestation and Forest Degradation (UN-REDD+) Programme emphasises the needs of individual countries and requires resolutions of 1 ha or better. Notwithstanding the sensitivity of Earth Observation (EO) data to biomass and the capability of retrieval models to infer biomass from EO observations, the requirements in Table 2 imply that the project should deliver data products at the highest possible resolution and also provide aggregates at coarser spatial resolution have better accuracy and precision than individual full spatial resolution pixels.

Table 2-1: Requirements for an AGB product formulated by the modelling and the policy communities as reported in the CCI BIOMASS URD. Requirements in bold are common to the two communities. Requirements in italic are community-specific (M for the modelling community, P for the policy community).

	Threshold (minimum) Requirements	Target (desired) Requirements
Product	**Map of aboveground biomass with associated precision.** This should be unbiased but if this cannot be achieved with current sensors, information on likely bias should be provided (M)	Map of aboveground biomass (and belowground biomass) with associated precision *and information on possible bias (M)* Map of biomass change with associated precision *and information on possible bias (M)*

Spatial Coverage	Global	**Global** with targeted/calibrated products for specific countries or other areas of interest (P)
Spatial Resolution	1 km x 1 km (M) 100x100 m / 1 ha or finer (P)	100 m resolution is desirable and 30 m resolution data could be used (M) 0,25-1 ha - resolution might vary depending on forest and ecosystem type, and country needs (P)
Temporal Extent	One time coverage for most recent period	2000-now
Temporal Resolution	Every 5 – 10 years (M) One time (P)	1 year (annual maps)
Reference System	Lat-Long (WGS-84) and equal-area projections	Lat-Long (M) Provided in country-specific reference grids (P)
Accuracy	Accuracy should be higher than existing maps. Continental-scale uncertainty estimation.	Data should be unbiased and with high precision at country level (P)
Delivery Mode	ftp for global products Web Service for regional products	ftp or Web Service and combined with training materials on how to use the data and within country capacity development (P)
Data Format	NetCDF for global products (M) GeoTIFF - for regional products (M)	NetCDF for global products (M) GeoTIFF - for regional products (M other country-preferred formats (P)
Other Requirements	Fully documented, transparent and standardised mapping methods Robust and standardised global validation scheme with protocol Metadata available Free and open access Full reporting of validation results and implications for product bias and precision (M)	Fully documented, transparent and standardised mapping methods Metadata available, Robust calibration and validation using available national data sources (i.e. NFI data) Access to underlying data in an accessible processing system *to produce their own data (P)* Free and open access Consistency with forest area change data Full reporting of validation results and implications for product bias and precision (P)

		Clear and transparent reporting of regional accuracy / uncertainty (P) Consistent spatial-temporal coverage (P)

Further interpreting the table of requirements, the data products by CCI BIOMASS described in this PUG fulfil all threshold requirements. Details are provided in Sections 3, 4 and 5, as well as in the Appendices. For the mapping methodology, refer to the Algorithm Theoretical Basis Document (ATBD) [RD-3] and the End-to-End ECV Uncertainty Budget (E3UB) [RD-4] documents.

2.3. Project outputs

The CCI BIOMASS project expands biomass mapping methodologies developed in the GlobBiomass project funded by ESA within the Data User Element (DUE). The GlobBiomass project (https://globbiomass.org) generated a global map of AGB with a spatial resolution of 100 m using multiple remote sensing observations from around the year 2010 (Santoro et al., 2020). CCI BIOMASS aims to a) generate annual global estimates of AGB for two current epochs (2017 and 2018), b) refine the 2010 data product derived in the GlobBiomass project, c) quantify AGB changes between epochs and d) prototype estimation of AGB in the mid-1990s.

This document presents the data products of the CRDP and an assessment in terms of their accuracy and reliability. The CCI BIOMASS data products (CRDPs) in year 3 consist of three global maps of AGB for the years 2010, 2017 and 2018, together with per-pixel standard deviation with a pixel size of 1 ha, i.e. for a 100 m x 100 m large area. The difference of AGB maps for two epochs, namely 2018 vs. 2010 and 2018 vs. 2017, together with an estimate of their standard deviation, forms the data product on AGB change. Each AGB change map is accompanied by a quality flag map, detailing the level of reliability of the AGB change estimate.

Estimates of AGB for the 1990s are not part of this data release.

Because of the different types of remote sensing data available for the three epochs, the AGB change maps may be affected by substantial biases. We strongly encourage referring to the quality flag layer to ensure that the data are used correctly (Section 4).

3. AGB Maps

3.1. Product description

The CCI BIOMASS project delivers spatially explicit estimates of AGB for three epochs and related standard deviations (SDs) as separate map products. The AGB product consists of global datasets with estimates of AGB (unit: tons/ha = Mg/ha). AGB is defined as the mass, expressed as oven-dry weight of the woody parts (stem, bark, branches and twigs) of all living trees excluding stump and roots. The AGB SD product is a separate data layer providing per-pixel SD of the AGB estimates in Mg/ha.

The data products currently provided by the project (year 3, Version 3.0) consist of three maps of AGB and AGB SD based on Earth Observation data acquired in 2010, 2017 and 2018, respectively. The spatial resolution of the map products is 100 m.

Figures 3-1 and 3-2 show the CCI BIOMASS AGB dataset of 2017 in Mg/ha and the corresponding map of SD. To enhance image contrast, the AGB map in Figure 3.1 has been clipped between 0 and 350 Mg/ha. The AGB SD map (Figure 3.2), expressed in the form of a relative SD with respect to AGB, has been clipped between 0% and 100% of the estimated AGB. For display reasons, AGB and AGB SD are shown for pixels labelled as forest according to the CCI Land Cover dataset of 2015 (version 2.07).

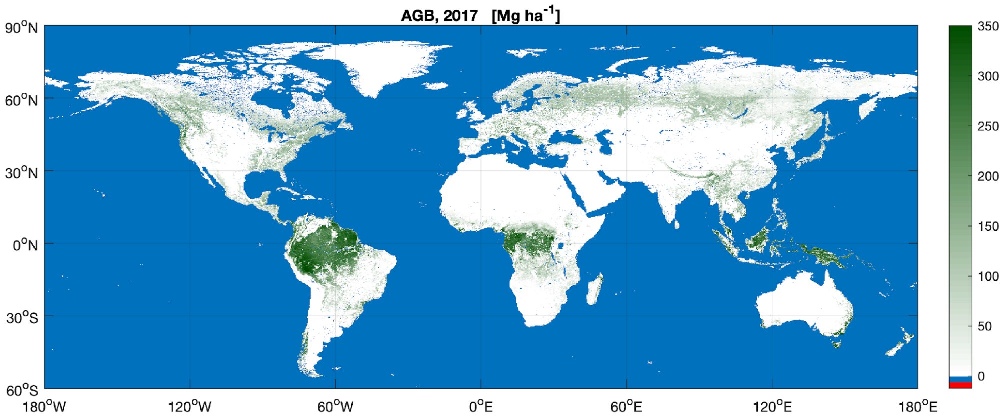

Figure 3-1: Global AGB estimates for the year 2017. Spatial resolution: 100 m.

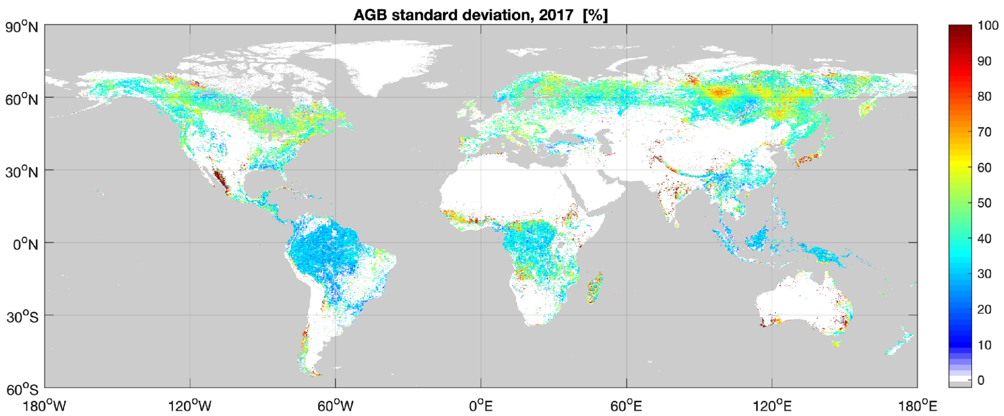

Figure 3-2: SD of global AGB estimates for the year 2017. Spatial resolution: 100 m.

Figure 3-3 shows two examples of AGB maps each covering an area of approximately 50 × 50 km^2, with the intention of highlighting the spatial details in the AGB dataset. Each AGB map can be compared with the corresponding image from Google Earth. The panels on the left hand side of Figure 3.3 show a forested region south of the Angara River in Central Siberia. Forests are dominated by boreal coniferous species with AGB up to 200 Mg/ha and the region has undergone intensive logging. Clear-cuts are clearly visible in the Google Earth image (yellow rectangles) and appear in the AGB map as white, i.e., with a value close to 0 Mg/ha. The panels on the right hand side of Figure 3.3 show a detail of the Amazonian forest along the Trans-Amazonian Highway, between the cities of Uruará and Altamira. While the forest north of the highway has been extensively logged to be replaced by agriculture, forests south of the highway are intact.

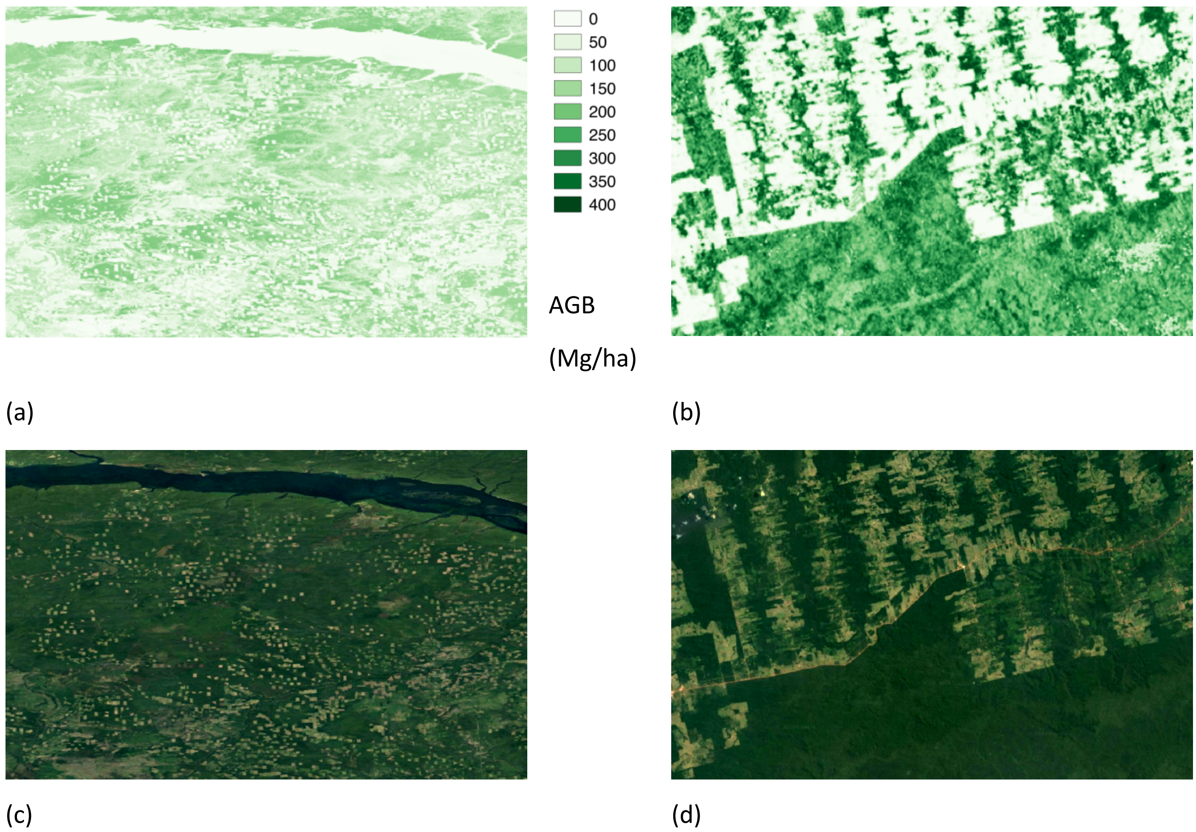

Figure 3-3: Detailed views of the AGB map for the region of Bratsk, Central Siberia, (a) and along the Trans-Amazonian Highway, between the cities of Uruará and Altamira, Brazil (b). Panels (c) and (d) are optical imagery from Google Earth and serve as reference for each of the AGB maps.

The 2010 and 2018 AGB datasets are not displayed in this Section because of their strong similarity in terms of AGB level and spatial distribution with the maps shown in Figures 3-1 and 3-2. Section 4 contains a quantitative assessment of the three datasets.

3.1.1. Processing chain

<u>EO datasets</u>

Since AGB is a variable inferred from measurements of structural parameters of a forest, a retrieval of biomass with remote sensing data needs to explore and exploit a large range of diverse observations. The need for a diversity of data sources is reinforced by the limited sensitivity of available spaceborne remote sensing observations to forest structural parameters.

Requirements on global coverage during each of the three epochs, open access to the data and sensitivity of the observations to forest structural parameters restricted the useful pool of remote sensing observations to images acquired by SAR C-band (Envisat ASAR for 2010 and Sentinel-1 for 2017-2018) and L-band (ALOS-1 PALSAR-1 for 2010 and ALOS-2 PALSAR-2 for 2017-2018).

The Sentinel-1 dataset consisted of images of SAR backscatter acquired during 2017 and 2018 over land between 75°N and 60°S. Sentinel-1 is a mission of the European Commission Copernicus initiative and consists of two units (1A and 1B) operating according to a predefined observation strategy that targets understanding and management of major environmental and societal challenges. Sentinel-1 images acquired in the Interferometric Wide Swath (IWS) mode were used. Some isolated gaps in North America were filled with images acquired in the Extended Wide Swath (EWS) mode [RD-3]. The two Sentinel-1 units became operational in spring 2017, which means that the density of observations was higher in 2018 than in 2017. All images were terrain-geocoded, speckle filtered and corrected for terrain-induced distortions [RD-3]. As a trade-off between processing speed, preservation of features and fulfilling the requirements on spatial resolution of an AGB product (see Section 2), each Sentinel-1 image was processed from the original 20 m to 150 m pixel size.

The ALOS-2 PALSAR-2 dataset consisted of terrain geocoded mosaics of the SAR backscatter acquired in Fine Beam Dual- polarization (FBD) and Wide Beam (WB) modes between 2017 and 2018 [RD-3]. The FBD mosaic consists of a single global dataset of the SAR backscatter per year. The WB mosaics covered the tropics only and were produced on a repeat-pass cycle basis, i.e., every 46 days. While the WB mosaics were provided with a pixel spacing of 100 m, the FBD mosaics were provided with a pixel spacing of 25 m. To be consistent with the hectare scale at which the Sentinel-1 and the WB mosaics were processed, the FBD mosaics were averaged to 100 m. All mosaics were produced by the Japan Aerospace Exploration Agency (JAXA) (Shimada and Ohtaki, 2010; Shimada et al., 2014). While the FBD mosaics are publicly available, the WB mosaics are available to members of the research community forming the Kyoto and Carbon (K&C) Initiative led and coordinated by JAXA's Earth Observation Research Center (EORC) (Rosenqvist et al., 2007). The K&C ScanSAR datasets are unique because they are tailored to support data needs raised by international environmental Conventions, Carbon Cycle Science, Climate Change and Conservation of the environment.

The overall quality of the SAR data for 2017 and 2018 was high and considered sufficient to generate a global dataset of AGB at hectare scale for 2017. Nonetheless, the ALOS-2 PALSAR-2 mosaics suffered from imperfect geolocation, banding and seams [RD-3], which resulted in some local errors when estimating AGB. Co-registration between datasets and balancing were used to reduce such systematic errors, but they could not be removed entirely. The impact on the estimates of AGB is discussed in Section 3.4.

The Envisat ASAR dataset consisted of terrain-geocoded images of SAR backscatter acquired in the Wide Swath Mode (WSM) between 2010 and 2011 [RD-3]. The dataset has a spatial resolution of 150 m, which is the reason for processing the higher resolution Sentinel-1 images to moderate resolution. The main drawbacks of the ASAR data are the lack of a cross-polarized channel and inhomogeneous coverage of terrestrial land surfaces. Dense sets of observations were achieved over northern regions, while most tropical and sub-tropical regions were not imaged frequently. This has practical implications for the 2010 AGB dataset (see below).

Similar to the ALOS-2 dataset, the ALOS-1 PALSAR-1 dataset consists of terrain-geocoded mosaics of SAR backscatter acquired in the FBD mode [RD-3]. WB mosaics were available but did not improve the quality of the AGB estimates based on the FBD data because of the lack of cross-polarized channel. Annual mosaics between 2007 and 2010 were produced by the Japan Aerospace Exploration Agency (JAXA) (Shimada and Ohtaki, 2010; Shimada et al., 2014). For the AGB data product of 2010, the cross-polarized mosaic of images acquired in 2010 was used, with occasional replacements with the 2009 dataset [RD-3]. As for the ALOS-2 mosaics, the ALOS-1 FBD mosaics were also averaged to 100 m.

Although for the three epochs the same kind of EO data were available (C- and L-band SAR backscatter), the difference in terms of observation density affected the accuracy of the AGB estimates. The 2010 dataset was based primarily on the single L-band SAR observation from the ALOS-1 mosaic except in areas of low AGB density where the retrieval algorithm weighted the C-band estimates more heavily than the L-band estimates. The 2017 and 2018 datasets used multiple observations of SAR backscatter at L-band and cross-polarized C-band images, both unavailable for 2010. This leads to improved estimates in the wet tropics and in low AGB regions [RD-6]. In addition, for regions where only one L-band observation was available, the AGB estimate was affected by the environmental conditions at the time of the single image acquisition. All these factors need to be considered when attempting any comparison of estimates between any of the three epochs.

AGB retrieval algorithm

The estimation of AGB is illustrated by the flowchart in Figure 3-4. Initially, separate algorithms (which share the same theoretical basis) were applied to the C-band and L-band datasets. With each algorithm, referred to as BIOMASAR, a global map of AGB was obtained. In year 2 (Version 2.0), direct estimation of AGB replaced the implementation of BIOMASAR in which the target variable was GSV (growing stock volume). This is because of the introduction of two allometries in the retrieval model that allowed a more explicit description of forest structural properties.

The BIOMASAR algorithm inverts a semi-empirical model relating the forest backscatter to canopy density and canopy height; these are replaced by two allometries relating canopy density to height (based on ICESat GLAS measurements) and canopy height to AGB (based on ICESat GLAS height metrics and global estimates of AGB, represented here by the GlobBiomass AGB dataset) [RD-3]. The model contains three parameters that are unknown a priori, and which correspond to specific backscatter components (ground, canopy) and backscattering properties of the forest. In order to estimate them, auxiliary datasets describing canopy density, microwave transmissivity, maximum biomass etc. are used. A detailed description of these data layers is available in the ATBD of the CCI BIOMASS project [RD-3]. Note that the model training phase does not require in situ observations, such as AGB plot data.

The two maps of AGB obtained from the BIOMASAR-C and BIOMASAR-L implementations, i.e., from the C- and L-band data, are merged using a set of weighting rules in order to reduce systematic estimation errors in one or the other map [RD-3]. Prior to merging, the BIOMASAR-C dataset of AGB is resampled from 150 m to 100 m to be compatible with the pixel spacing of the BIOMASAR-L dataset. In a nutshell, the weighting favours the BIOMASAR-L AGB estimates in regions of high AGB because of the weaker sensitivity of C-band backscatter to biomass in mature and dense forest. The AGB of younger and regrowing forest is often an average of the two values estimated by BIOMASAR-C and -L. In Appendix B, the maps with weights applied in the merging process are illustrated for 2010 and 2017 (Figures B2 and B3, respectively). Because of the different density of observations in 2010 and 2017-2018, the maps of the weights differ.

The shaded part in Figure 4 indicates that the estimation framework foresees the integration of additional AGB datasets. This will become relevant in the near future with a multitude of global AGB datasets planned for release as part of mission objectives (GEDI, NISAR, BIOMASS) or as part of currently ongoing activities to quantify biomass.

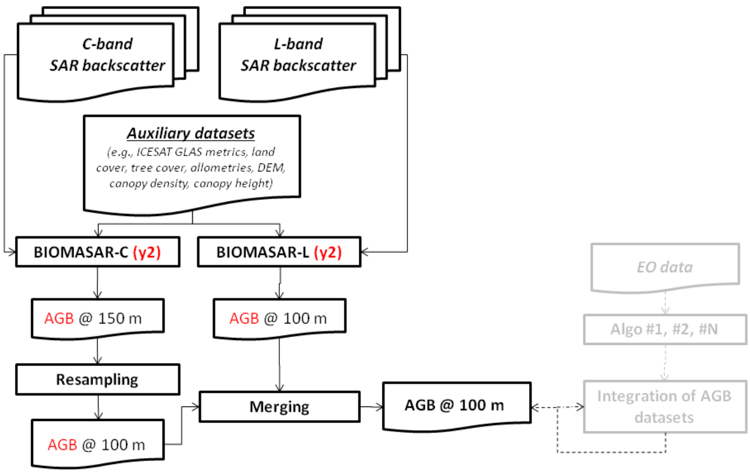

Figure 3-4: Functional dependencies of datasets and approaches forming the CCI Biomass global biomass retrieval algorithm in year 2. Text in red refers to changes to the retrieval algorithm introduced in year 2. The shaded part of the flowchart represents potential improvements following the implementation of additional retrieval techniques.

The AGB map is accompanied by a per-pixel estimate of its SD, which is computed by propagating individual uncertainties in (i) the SAR measurement, (ii) the modelling framework behind the BIOMASAR algorithms and (iii) the merging procedure. Full characterization of the SDs is provided in the E3UB report [RD-4].

3.1.2. Specifications of data products

Spatial coverage: global

Validity of estimates: Estimates have been generated for each point on Earth for which the remote sensing data were available.

Urban areas, ice-capped surfaces and bare soils according to the Copernicus Global Land service land cover datasets of the same year (Buchhorn et al., 2019; available at https://land.copernicus.eu/global/products/lc), have been re-mapped to 0 Mg/ha. For the 2010 AGB dataset, the 2015 land cover dataset was used.

Reference system: Lat-long, WGS-84

Corner coordinates: top left corner of pixel

Pixel spacing: The AGB and AGB SD estimates are provided with a pixel spacing of 0.0008888° (roughly corresponding to 100 m at the Equator).

Timeframe: years, 2010, 2017 and 2018

Data format: NetCDF (one global file) and GeoTiff (10° × 10° tiles)

3.1.3. Format of the NetCDF file

Naming Convention

The filename convention of the global AGB and AGB SD maps delivered by the CCI BIOMASS project is the following:

Filename = <id>-fv<version>.nc

where <id> = <project>-<level>-<var>-<code>-<spatres>-<epoch>

The dash "-" is the separator between name components. The filename convention obeys NetCDF Climate and Forecast (CF) conventions by using the postfix ".nc". The different name components are defined in Table 3-1.

Table 3-1: Elements of the NetCDF file name of the CCI BIOMASS AGB and AGB SD data products delivered by the CCI BIOMASS project.

Field	Signification	Value
Project	Project acronym	ESACCI- BIOMASS (constant)
Level	Processing level	L4 (constant)
Var	Unit of the product	AGB
code	Product code identifier	MERGED (constant)
spatres	Spatial resolution	100 m (constant)
epoch	Year of the product	2010, 2017 or 2018
version	Incremental that follows the successive revisions of the CCI-BIOMASS processing lines	Version of product revision, preferably major.minor, optionally with processing centre [a-zA-Z0-9._]*

The file names of the global AGB maps in NetCDF format distributed with the CRDP of year 3 are:

ESACCI-BIOMASS-L4-AGB-MERGED-100m-2010-fv3.0.nc

ESACCI-BIOMASS-L4-AGB-MERGED-100m-2017-fv3.0.nc

ESACCI-BIOMASS-L4-AGB-MERGED-100m-2018-fv3.0.nc

Each NetCDF file contains the AGB (16-bit integer), AGB_SD (16-bit integer), latitude (64-bit floating point), longitude (64-bit floating point) and time (64-bit floating point) information.

Format

The AGB maps are delivered in NetCDF-4 format. The NetCDF files specification follows CF conventions (ESA Climate Office, 2019).

Metadata

The metadata for the AGB maps are provided as global attributes in the NetCDF file. The metadata follow the CCI guidelines (ESA Climate Office, 2019).

Estimated size

The size of each annual AGB dataset, including the SD layer, in NetCDF format is approximately 18 GB.

3.1.4. Format of the GeoTiff tiles

Naming Convention

The filename convention of the AGB and AGB SD tiles delivered by the CCI BIOMASS project is the following:

Filename = <id>-fv<version>.tif

where <id> = <N/S flag><Latitude><E/W flag><Longitude>_<project>-<level>-<var>-<code>-<spatres>-<epoch>

The dash "-" is the separator between name components. The different name components are defined in Table 3-2.

Table 3-2: Elements of the GeoTiff file name of the CCI BIOMASS AGB and AGB SD data products delivered by the CCI BIOMASS project.

Field	Signification	Value
N/S flag	North/South hemisphere of northernmost row in the tile	N or S
Latitude	Northernmost latitude coordinate of tile	Integer (2 digits, between 00 and 80)
E/W flag	East/West hemisphere of westernmost column in the tile	E or W
Project	Westernmost longitude coordinate of tile	Integer (3 digits, between 0 and 180)
Project	Project acronym	ESACCI- BIOMASS (constant)
Level	Processing level	L4 (constant)
Var	Unit of the product	AGB or AGB_SD
code	Product code identifier	MERGED (constant)
spatres	Spatial resolution	100 m (constant)
epoch	Year of the product	2010, 2017 or 2018
version	Incremental that follows the successive revisions of the CCI-BIOMASS processing lines	Version of product revision, preferably major.minor, optionally with processing centre [a-zA-Z0-9._]*

For the specific case of a tile covering the area between (60°N, 40°E) and (50°N, 50°E), the file names of the AGB maps in GeoTiff format distributed with the CRDP of year 3 are:

N60E040_ESACCI-BIOMASS-L4-AGB-MERGED-100m-2010-fv3.0.tif

N60E040_ESACCI-BIOMASS-L4-AGB-MERGED-100m-2017-fv3.0.tif

N60E040_ESACCI-BIOMASS-L4-AGB-MERGED-100m-2018-fv3.0.tif

Accordingly, the file names of the SD layer are

N60E040_ESACCI-BIOMASS-L4-AGB_SD-MERGED-100m-2010-fv3.0.tif

N60E040_ESACCI-BIOMASS-L4-AGB_SD-MERGED-100m-2017-fv3.0.tif

N60E040_ESACCI-BIOMASS-L4-AGB_SD-MERGED-100m-2018-fv3.0.tif

Estimated size

For each of the three epochs, the Geotiff dataset consists of approximately 11 GB of AGB estimates and 11 GB of AGB SD estimates.

Format

Short unsigned integer (uint16).

3.1.5. Format of the data product – additional information

Additional information on the data products are reported below. These are independent from the format in which the maps are stored.

Product layers

AGB and AGB SD. Both are expressed in Mg/ha.

Processing Level

Level 4 (i.e. “variables that are not directly measured by the instruments, but are derived from these measurements” according to CEOS, 2008)

Units

Each pixel value of the AGB corresponds to a number expressed in Megagrams per hectare (Mg/ha). Valid AGB values are between 0 and 10,000 Mg/ha.

Each pixel value of the AGB SD corresponds to a number expressed in Megagrams per hectare (Mg/ha). Valid AGB SD values are between 0 and 10,000 Mg/ha.

Spatial Extent

All terrestrial zones of the Earth between 90°N and 60°S.

Spatial Resolution

0.0008888°, corresponding to nearly 100 m at the Equator

Temporal resolution

Annual

Projection

The Coordinate Reference System (CRS) is a geographic Lat/Long coordinate system (EPSG: 4326) based on the World Geodetic System 84 (WGS84) reference ellipsoid. The projection specifications consist of semi-major axis (6378.14 km), semi-minor axis (6356.76 km) and inverse flattening parameter (298.26 m). The latitude and longitude coordinates are specified in decimal degrees. A complete description of the CRS is given as an ISO 19111 WKT representation (Table 3-3).

Table 3-3: Description of the coordinate reference system defining the global AGB products.

```
GEOGCS["GCS_WGS_1984",
    DATUM["D_WGS_1984",
        SPHEROID["WGS_1984",6378137.0,298.257223563]],
    PRIMEM["Greenwich",0.0],
    UNIT["Degree",0.0174532925199433],
AUTHORITY["EPSG",4326]]
```

3.2. Qualitative assessment

The level of detail of the CCI BIOMASS maps of AGB has been discussed in Section 3. Each of the three CCI BIOMASS maps provides a wall-to-wall portrait of AGB for the corresponding year (2010, 2017 and 2018). The maps reproduce the patterns of biomass distribution on Earth (Figure 3-1). The highest AGB (> 300 Mg/ha) is found in the wet tropics of South America, Africa and Southeast Asia, and in the temperate rainforest of the Pacific Northwest between Canada and the U.S., southern Australia and along the Andes between Chile and Argentina. The map in Figure 3-1 shows a clear gradient of biomass for decreasing latitude in the northern hemisphere, following the transition from boreal to temperate and tropical forest. In the southern hemisphere, AGB drops from tropical wet to tropical dry forest and savannah vegetation. AGB increases markedly at the southernmost latitudes corresponding to temperate cool forests.

The SD of the AGB estimates in Figure 3-2 depends on the proportion of C- and L-band estimates. For the wet tropics, where the estimate depends solely on L-band data, the SD is about 40% of the estimated AGB. In the boreal zone, the effect of the weighting becomes quite evident. The SD in regions where the AGB estimate is based primarily on C-band (northern and southern boreal and temperate forests, dry tropics of the southern hemisphere) is slightly higher, at about 50% of the estimated value. The reason for the high SD for the C-band based estimates of biomass is the weak sensitivity of the backscatter to biomass and the strong temporal correlation of the retrieval errors so that the multi-temporal combination of individual AGB estimates implemented in BIOMASAR reduces the uncertainty only to a certain extent. The largest SD (about 80-100% of the estimated value) occurs in regions where C-band was favoured but the number of backscatter observations used to estimate AGB was low (around 10).

3.3. Validation

Validation refers to a comparison of the map value of AGB with an independent dataset of measurements that can be considered to act as reference for the true AGB. Forest field inventory measurements with well-known and well-described reporting protocols represent the primary source for validation. Validation of the three AGB maps is described in the Product Validation & Intercomparison Report (PVIR) [RD-6]. Validation confirmed the visual impression that the spatial distribution of AGB is well captured globally, especially when considering reference measurements covering an area comparable with the size of a pixel in the map, e.g. approximately 1 ha (Figure 3.5). The agreement between map and reference AGB averages in the 2017 and 2018 datasets was expected, given that the same set of predictors was used to estimate AGB (ALOS-2 and Sentinel-1 multi-temporal observations of the SAR backscatter). The slightly better agreement between map and reference AGB averages for 2017 and 2018 compared to 2010 is due to the poorer observational dataset available for 2010.

Each of the three maps displays increasing variance but limited bias for AGB up to 350 Mg ha^{-1}. Thereafter, the maps tend to underestimate AGB. The underestimation is a consequence of the limited sensitivity of the EO observables to AGB, the constraint applied in the inversion to a maximum AGB that is lower than in reality (see PVASR) and the need to strongly filter the input ALOS-2 data to avoid artefacts. The overestimation at around 250 Mg ha^{-1} corresponds primarily to the CoFor plots (Ploton et al., 2020) and Southwest Australia. The underestimation above 400 Mg ha^{-1} occurs in Tasmania. In both cases, the discrepancy between map-based and plot-based averages is explained by the maximum AGB set to constrain the retrieval within a range of plausible values. Over and under-estimation occurs when the maximum AGB is set either too high or too low. For the current version of the CCI maps, the maximum AGB was based on an allometric function that relates canopy height (from spaceborne LiDAR) and AGB (from map-based values of the GlobBiomass dataset). In [RD-3], we noted that if the LiDAR coverage does not include the forests with the highest densities, the maximum AGB is missed (e.g., in Tasmania). Also, a number of assumptions were needed to reduce the impact of biases in the GlobBiomass dataset on the allometries.

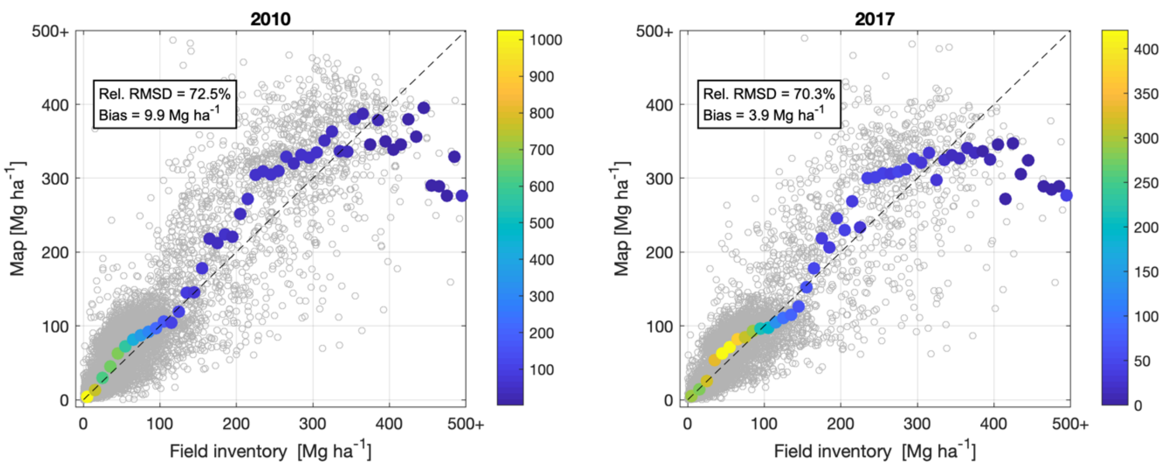

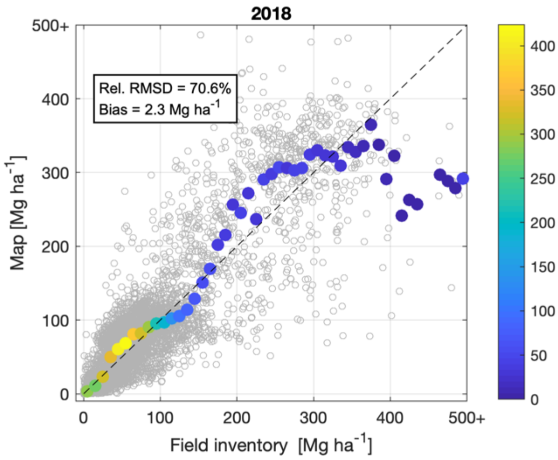

Figure 3-5: Scatterplots of average AGB from in situ data (x axis) and corresponding values from the AGB map (y axis) using a 0.1° (i.e., 10 km) grid for each of the three AGB maps (year 3, Version 3.0). In each scatterplot, the coloured circles represent the average map value for binned reference AGB (10 Mg/ha wide intervals). The colour represents the number of grid cells within a specific bin. The scatterplots are based on data provided by Wageningen University and used to compile the CCI BIOMASS PVIR [RD-6].

One of the intrinsic limitations of validation with inventory data is that the inventory samples are an opportunistic collection of measurements gathered for other reasons than validating AGB estimates from remote sensing data. Hence, trends identified by the validation need to be understood before coming to conclusions.

The same concept applies if the source of reference AGB measurements is a high-resolution map. Nonetheless, before applying the map in local to regional- scale applications, users may want to evaluate the accuracy of the map in their own area of interest, for instance with the aid of locally available in situ information on AGB. A frequent scenario may be that forest inventory data collected from small diameter plots (e.g., 10-20m diameter) are used, despite the mismatch with respect to the spatial resolution of the CCI AGB maps (100 m x 100 m). It is then important to understand that (i) this spatial mismatch poses limits on the possibility to quantify the local error and overall bias of the CCI AGB maps and (ii) comparisons of map and in situ AGB estimates need to be interpreted with caution.

With the aid of airborne laser scanner (ALS) derived AGB maps, we demonstrate below the limitations associated with assessing the precision and bias of a coarser resolution AGB map (such as the CCI AGB map with 100x100 m^2 resolution) using a sparse network of plot-level inventory data where plots cover only a small fraction of the corresponding pixel in the AGB map. Specifically, we demonstrate that the error associated with comparing AGB estimates in the 1 hectare map with AGB information collected in smaller plots is revealed not only in the form of underestimation of the map precision, but also in a false representation of the bias of the AGB estimates. We here focus on this sampling-related error and do not consider additional error sources such as geolocation and measurement errors in the in situ data or the allometric equations used to estimate from AGB at plot level.

The AGB maps considered here were produced from ALS data acquired over two forest sites in Remningstorp, Sweden, and Lope, Gabon, i.e., a boreal and a tropical forest site. Both ALS datasets were acquired in the frame of the airborne ESA BIOSAR (Ulander et al., 2011) and AfriSAR (Hajnsek et al., 2017) campaigns to provide detailed information on the forest's vertical structure and to produce high-resolution AGB maps. The maps, with a spatial resolution of 20 m (Figure 3.6), cover an area of 22 km^2 (Remningstorp) and 52 km^2 (Lope), respectively. For further information on how the maps were produced, the reader is referred to the references cited above.

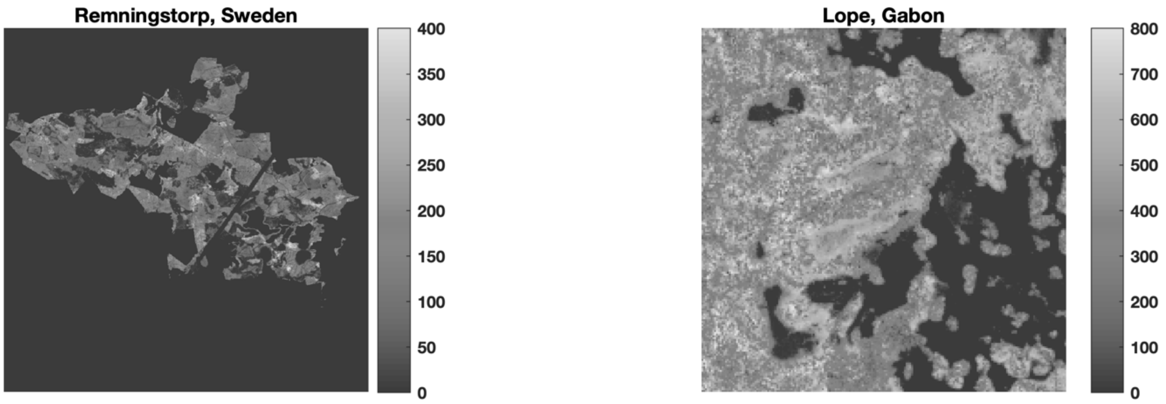

Figure 3-6: AGB maps with a resolution of 20 m × 20 m derived from ALS data acquired over the test sites Remningstorp, Sweden, and Lope, Gabon.

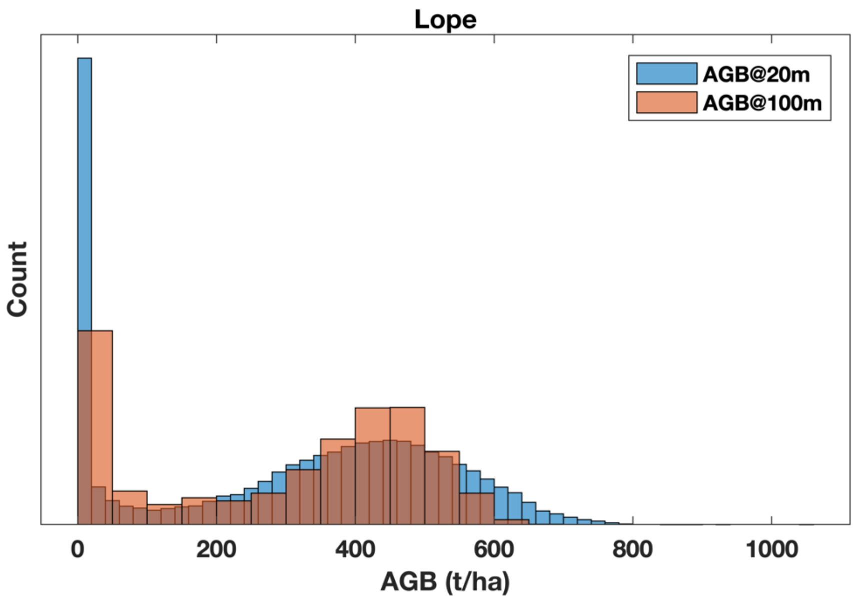

Figure 3-7: Histograms of AGB in Lope at 20 m × 20 m and 100 m × 100 m pixel size.

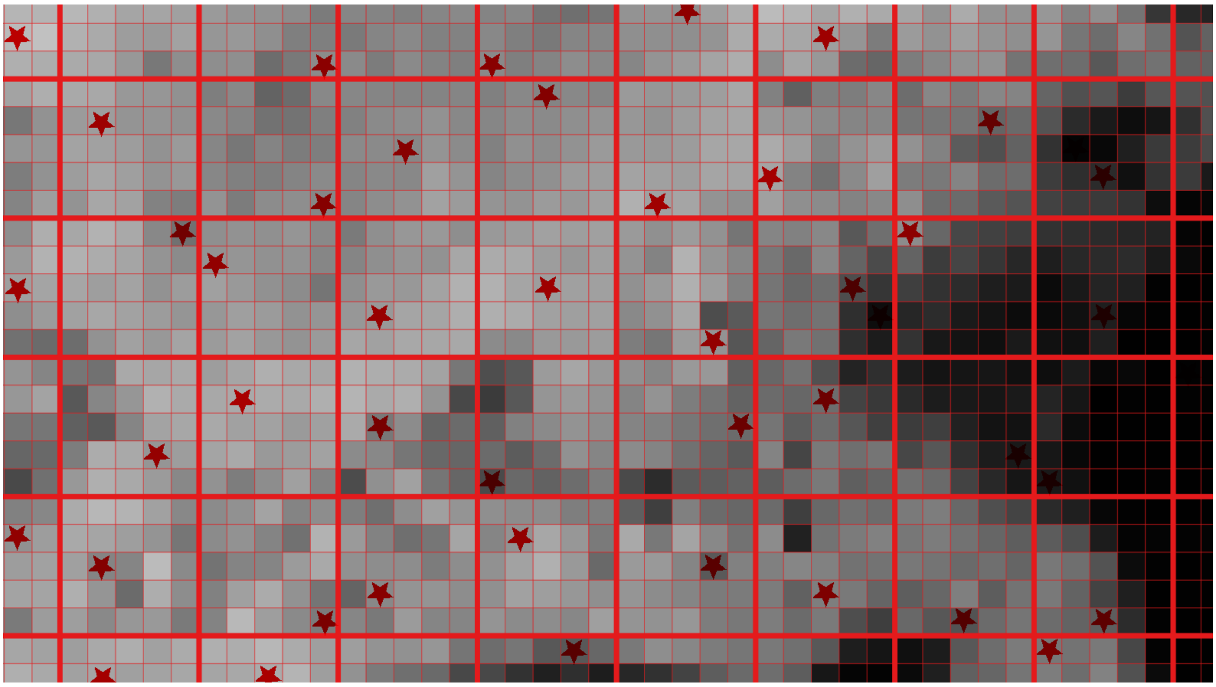

Figure 3-8: 20 m × 20 m pixel grid of an ALS-derived AGB map nested into a 100 m × 100 m pixel grid representing the global AGB map. The 20 m pixels labelled with a star are used to simulate 20 m plot level AGB information for evaluating the errors in the 100 m AGB map.

The ALS AGB maps are used to simulate a scenario in which hectare-scale AGB estimates from Earth Observation data are validated using sub-hectare scale reference information. This is achieved by first aggregating the ALS-derived maps from 20 m x 20 m to 100 m x 100 m pixel size. The histograms of AGB at 20 and 100 m scale are illustrated in Figure 3.7 for Lope. The aggregation leads to differences in the observed range of AGB values, in particular with respect to the maximum AGB. At 20 m scale, the maximum AGB around 800 t/ha; at 100 m scale AGBs rarely exceed 600 t/ha. Subsequently, any of the 20 m pixels located within a 100 m pixel is treated as if it were a plot used to evaluate the error of the 100 m map. For Lope, plotting the AGB in the 100 m map against a randomly selected 20 m pixel inside each 100 m pixel (indicated in Figure 3.8) yields the scatterplot in Figure 3.9. The RMS error is of order 100 t/ha (30% of the mean AGB) and there are deviations from the 1:1 line that depend on the AGB level. These deviations are systematic and not limited to a given test site, as is clear when repeating the comparison for 100 random samples of 20 m x 20 m and plotting the 100 m AGB against the 20 m AGB as curves that reflect the mean trend (average 100 m AGB in 20 t/ha intervals of against the 20 m AGB) (Figure 3.10). Despite the 100 m maps simply representing the averaged version of the 20 m map, the comparison suggests that the 100 m map is biased, in that low AGB ranges seem to be overestimated and high AGB ranges underestimated.

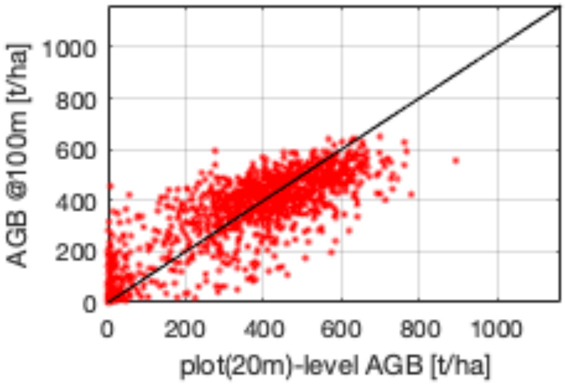

Figure 3-9: AGB estimates at 100 m × 100 m scale vs. sub-pixel random samples of AGB at 20 m × 20 m scale.

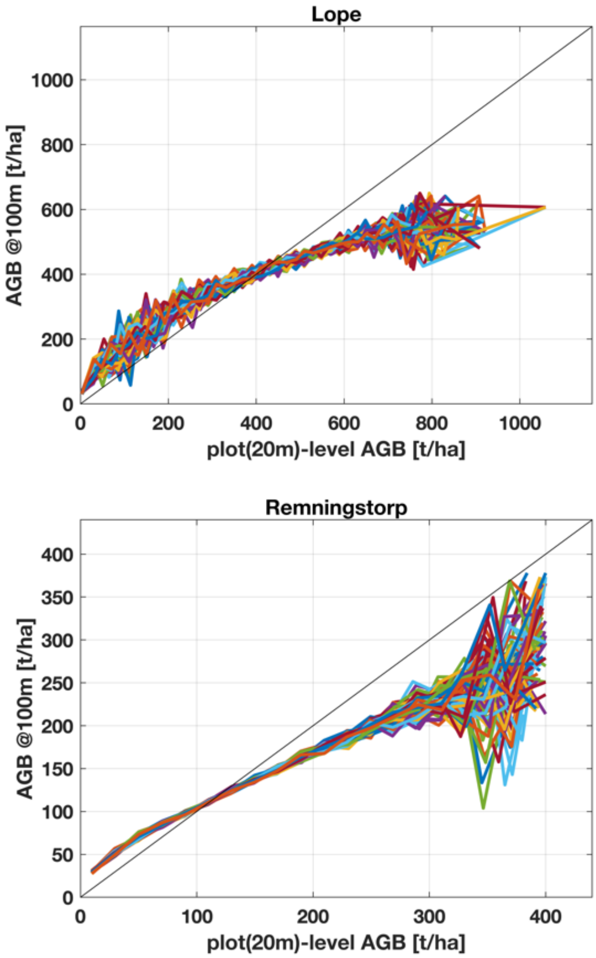

Figure 3-10: 100 m AGB plotted vs. sub-pixel samples of AGB at 20 m scale in Lope and Remningstorp.

This false indication of bias may be compensated by using more than one random sub-sample of 20 m AGB pixels per 100 m AGB pixel (Figure 3.11). Forest inventory data are generally not collected at such high spatial density. However, when, for example, comparing AGB maps with reference AGB information derived from small-footprint LiDAR, such a strategy may be feasible.

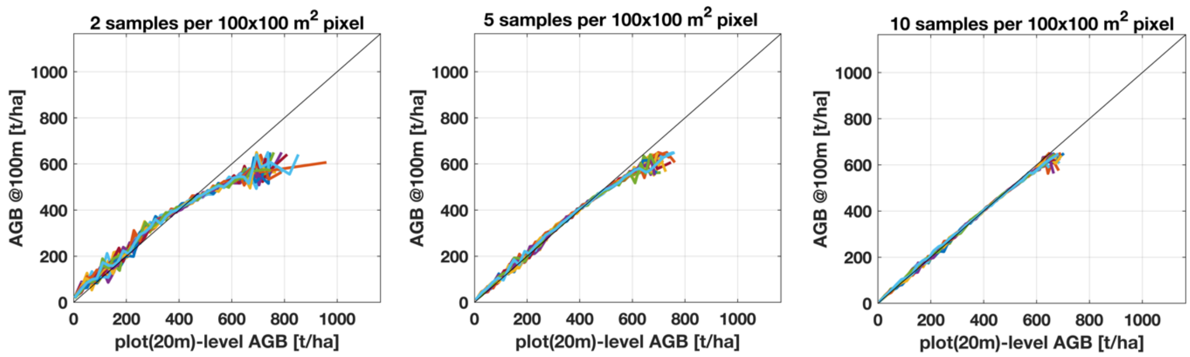

Figure 3-11: 100 m AGB plotted vs. sub-pixel samples of AGB at 20 m in Lope and Remningstorp when averaging for each 100 m AGB pixel more than one (two, five, ten) 20 m AGB pixels.

To build up confidence in the CCI BIOMASS AGB estimates, an additional comparison with estimates of AGB from ALS data and part of a dataset of in situ measurements of CCI BIOMASS is reported. Data available from the Sustainable Landscapes Brazil project (Longo et al., 2018), the Carbon Monitoring System (CMS) Kalimantan project (Ferraz et al., 2018) and the United States National Ecological Observatory Network (NEON) (https://data.neonscience.org/home) program were processed by Nicolas Labriere and Jerome Chave, at EDB Toulouse, to generate LiDAR-based maps of AGB with a pixel size of 100 m x 100 m. Although laser-based estimates are themselves estimates of AGB and therefore do not qualify as reference, they cover regions not represented in the plot inventory database and provide valuable indications with respect to potential systematic errors in the AGB retrieved in CCI.

Figure 3-12 shows scatterplots comparing ALS-based and map-based estimates of AGB at the level of individual pixels, each pixel covering 1 ha. To aid interpretation, we also included median values per AGB bins of the ALS-based values and inter-quartile ranges of the map-based AGB per AGB bin. For the Brazilian and U.S. datasets the comparison is undertaken at sites for which LiDAR data were acquired in the same year as the CCI datasets (Brazil: 13 sites in 2017 and 14 in 2018; U.S.: 33 sites in 2017 and 27 in 2018). The CMS dataset of Kalimantan was acquired in 2014 and is compared with the map-based estimates of 2017 (86 sites). Overall, the spatial distribution of AGB is captured but the scatterplots show large variance of the estimated AGB and, for the tropical sites, a tendency to first over- and then underestimate AGB for increasing AGB. Overestimation typically occurs in mixed landscapes of primary and secondary forest. We associate overestimation with an imperfect representation of the maximum AGB, this being a result of the allometry relating height to AGB being tailored to undisturbed forest. Underestimation both in Brazil and Kalimantan was explained by the imperfect allometry between height and AGB, which in our case was set to predict substantially smaller AGB than the allometry (based on in situ measurements) used to convert the LiDAR top-of-canopy height to AGB. Overall, however, the strong biases particularly evident in Kalimantan are caused by the rather simple modelling framework and the assumptions behind the model training that do not allow capture of the small-scale heterogeneities of the landscape described in Ferraz et al., 2018. For the U.S. sites, the agreement is better than for the tropical sites because of the correctly estimated allometries and, thereof, the maximum AGB. For the Australian sites, the agreement between map and LiDAR pixels confirms the trend identified with the plot-based averages. For AGB > 300 Mg ha^{-1} the map underestimates AGB, which again we attribute to the maximum AGB, which was set too low compared to the values estimated from the LiDAR data.

Sustainable Landscapes Brazil

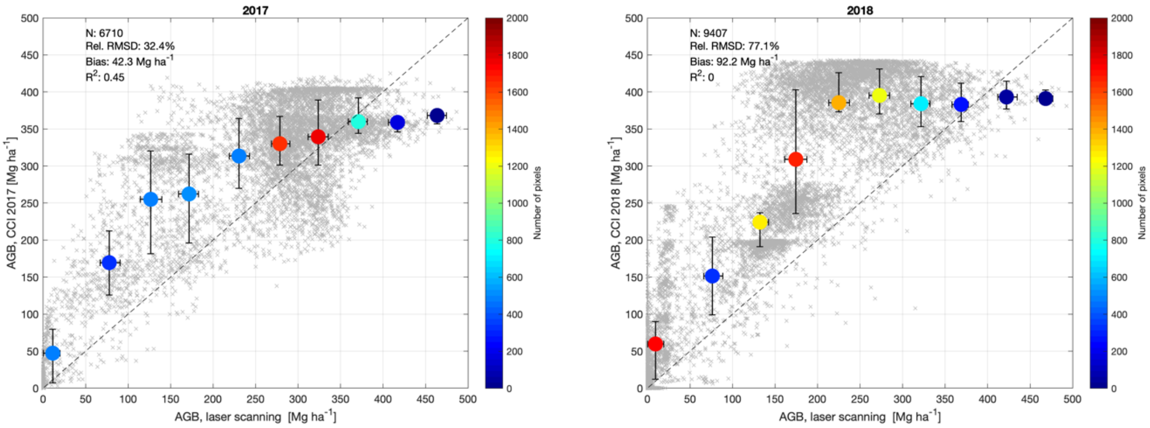

U.S. NEON program

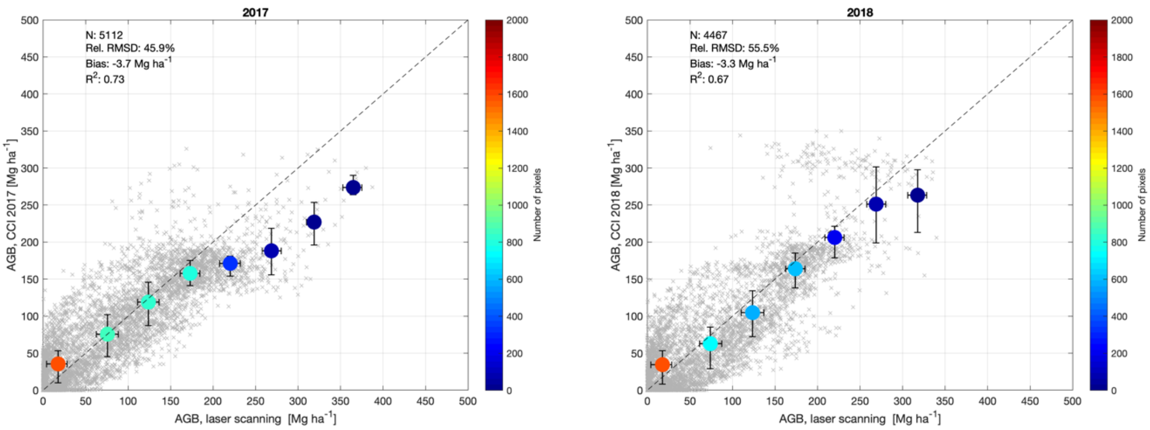

CMS Kalimantan

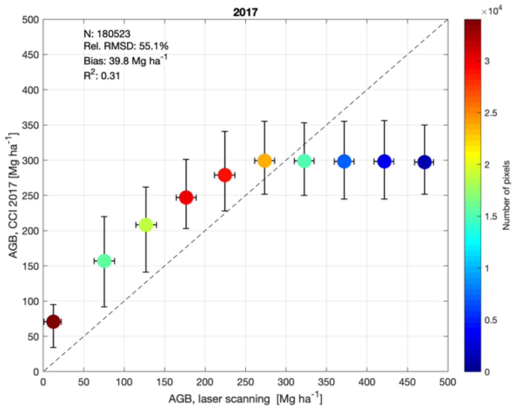

TERN Australia

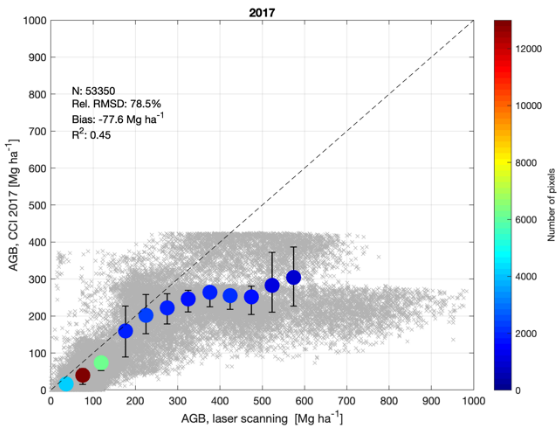

Figure 3-12: Scatterplots comparing LiDAR-based AGB and estimated AGB. The coloured circles and the bars represent the median and inter-quartile ranges of AGB for 50 Mg ha-1 wide bins. Retrieval statistics reported in this figure include the number of pixels, relative RMSD, bias and R^2 coefficient of determination.

3.4. Limitations

As a result of the validation process and additional analysis undertaken with averages at administrative level (not reported in this document), limitations of the CCI BIOMASS datasets of AGB can be grouped into two major categories: signal-dependent and processing-dependent. The signal-dependent limitations relate to the fact that the EO data used to estimate AGB are only indirectly related to biomass and therefore several assumptions need to be made when attempting to obtain an estimate of AGB from the observations. This aspect is discussed under “local biases”. The second type of limitation is a direct consequence of imperfections at the level of data processing, i.e., errors introduced into the remote sensing image by the data provider. These errors can be local and global. A description of errors affecting the remote sensing data is provided in the ATBD [RD-3]. The effect of local errors can be easily spotted in the AGB dataset and is discussed under “seams” and “topography” separately. The impact of inaccurate geolocation on the AGB estimates is harder to demonstrate and is, therefore, not presented in this document.

3.4.1. Local biases

An AGB estimate based on C- and L-band backscatter is prone to errors and large inaccuracy in regions where the backscatter has limited sensitivity to biomass. This is typically the case in moderate to high biomass forest (i.e., for large biomass density) and when the environmental conditions alter the SAR backscatter so that the sensitivity to biomass is completely lost (e.g., under wet conditions). Specific environmental conditions can introduce an overall bias in the estimates of AGB. One way to overcome such issues is to retrieve AGB using multiple observations. In the CCI BIOMASS retrieval algorithms, multiple observations of C-band backscatter (from Sentinel-1 and Envisat ASAR) and several mosaics of L-band backscatter (from ALOS-1/2 and PALSAR-1/2) are used whenever possible, to reduce noise and errors. Still, at the level of a single pixel, the error can be very large. Even aggregates may be biased if the retrieval did not perform well (e.g., insufficient number of observations, incorrect parameterization of algorithm). As shown by the dispersion of the data points in Figure 3.5, the CCI BIOMASS dataset shows both under- and overestimation but these do not occur similarly at all locations. We give a brief summary of areas prone to errors and their explanation below

- Underestimation for AGB > 300-400 Mg/ha (depending on region). In dense tropical rainforest, the AGB here is based purely on L-band backscatter because of the lack of sensitivity of C-band to AGB. The extremely weak sensitivity of L-band backscatter to biomass and the conservative rules implemented in the BIOMASAR algorithm to estimate biomass partly explain this [RD-3]. We also identified an issue with the height-to-AGB allometry implemented in the retrieval algorithm, which appears to generate lower AGB estimates than the allometry recently derived from the LiDAR datasets in Brazil and Kalimantan. The same issue was identified in Australia. The effect of topography on backscatter and thus on the estimated AGB should have been reduced compared to past mapping efforts because of its explicit inclusion in the retrieval model. Nonetheless, we still observe underestimation in local areas characterized by moderate to strong topography where the models used to compensate for distortions of the SAR backscatter due to sloped terrain were not correct.
- Overestimation is usually a local feature due either to an incorrect setting of the maximum AGB or of the allometry relating AGB to canopy height. Although based on multiple observational datasets [RD-3], the maximum AGB layer does not account for small-scale discontinuities corresponding to transitions in forest cover. A more detailed characterization of AGB discontinuities is required in order to improve the spatial characteristic of this layer. While a global allometry between height and AGB does not yet exist, we relied on the GlobBiomass AGB dataset (in the range of values found to be accurately estimated) but then used a coarse resolution to characterize the power-law function relating AGB to canopy height estimated from global LiDAR measurements. The coarse resolution and local biases in the AGB map cause the allometry to be locally biased. Continual advances in characterizing the allometry between LiDAR height metrics and AGB coupledwiall help to improve the allometry implemented in the CCI BIOMASS retrieval models.

3.4.2. Seams

Seams are unnatural AGB variations that are related to the imagery. The origin of the seams in the CCI BIOMASS dataset was identified in the ALOS-2 and ALOS-1 mosaics over the tropics, where images acquired on different dates and seasons were stitched together to obtain global coverage. Images acquired at different times may have strong radiometric differences. In this case, the feathering is sub-optimal, introducing radiometric offsets between one image and the adjacent one. Although SAR pre-processing tried to reduce such seams [RD-3] and the models used to retrieve biomass are strongly spatially adaptive [RD-3], some of the seams remained at the end of the processing chain. In particular, these become visible in regions of weak sensitivity of the backscatter to biomass (e.g., dense tropical forest) and where AGB was based only on the L-band mosaics. Seams appearing in the form of a small radiometric offset (of the order of 0.1-0.2 dB) translate to a clear biomass offset > 10 Mg/ha and show up as unnatural features (Figure 3-13).

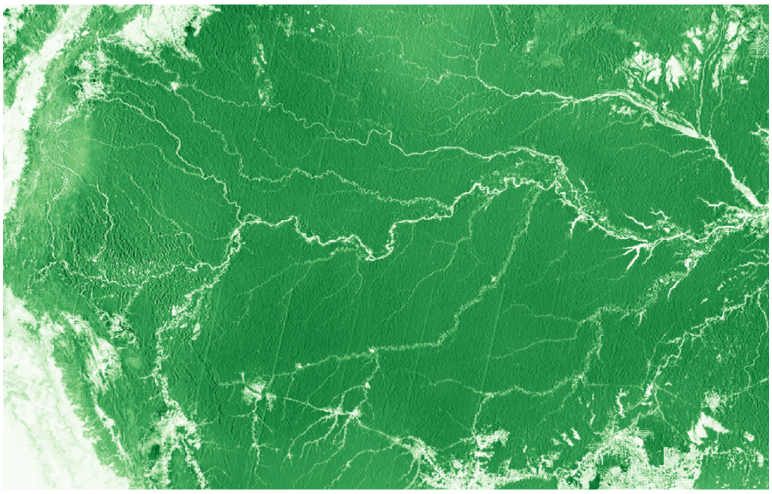

Figure 3-13: Example of seams in the AGB dataset appearing as diagonal bright lines. AGB in this region (western Amazon) was based on the ALOS-2 PALSAR-2 mosaic only and the seams correspond to the point of intersection of two adjacent strips of data.

The Sentinel-1 datasets are also affected by seams corresponding to the original data. Seams are mostly visible in Southeast U.S. and Southeast China, where the AGB estimates were almost exclusively based on S-1 images.

The seams tend to disappear when averaging to coarser resolution, e.g., 1 km or more, which however does not exclude that they may have an impact on the spatial characterization of AGB changes.

3.4.3. Topography

The retrieval of biomass was based on images of SAR backscatter, which are affected by geometric distortions due to the side-looking configuration of the radar instrument. Sloped terrain facing the radar is characterized by stronger backscatter than sloped terrain looking away from the radar. If untreated in the pre-processing, this would cause AGB estimates to be systematically higher on the slopes facing the radar. Both the ALOS-1/2 mosaics and the ASAR / Sentinel-1 images were treated to compensate for slope-induced distortions of the backscatter [RD-3] and ideally the backscatter after compensation should be the same regardless of the orientation of the terrain. In practice, imperfections in the Digital Elevation Model (DEM) used to mimic the terrain slope and assumptions made to simplify the correction procedure result in a residual slope-induced backscatter error which translates into incorrect AGB values.

Although we have introduced a model-based framework to adjust the backscatter to local incidence angle as a function of canopy cover [RD-3], topography-induced distortions in the map of AGB are still visible whenever the model was not able to capture the relationship between these variables (poor correspondence) or because of errors in the DEM or the canopy cover dataset used as reference. Figure 3-14 shows an example of AGB estimates affected by residual topographic effects. All slopes facing the radar (observing in this case from the left-hand side) have higher AGB than slopes looking away from the radar. The impact of slope-induced biases on AGB was particularly evident in the wet tropics where AGB was based solely on ALOS-2 PALSAR-2 mosaics for which the compensation for topography was undertaken with a simpler approach than in the processing applied to Sentinel-1 data. Given the poor estimates by Sentinel-1 in the wet tropics, it was preferred in the end to favour the ALOS-2 estimates in spite of topography-induced biases.

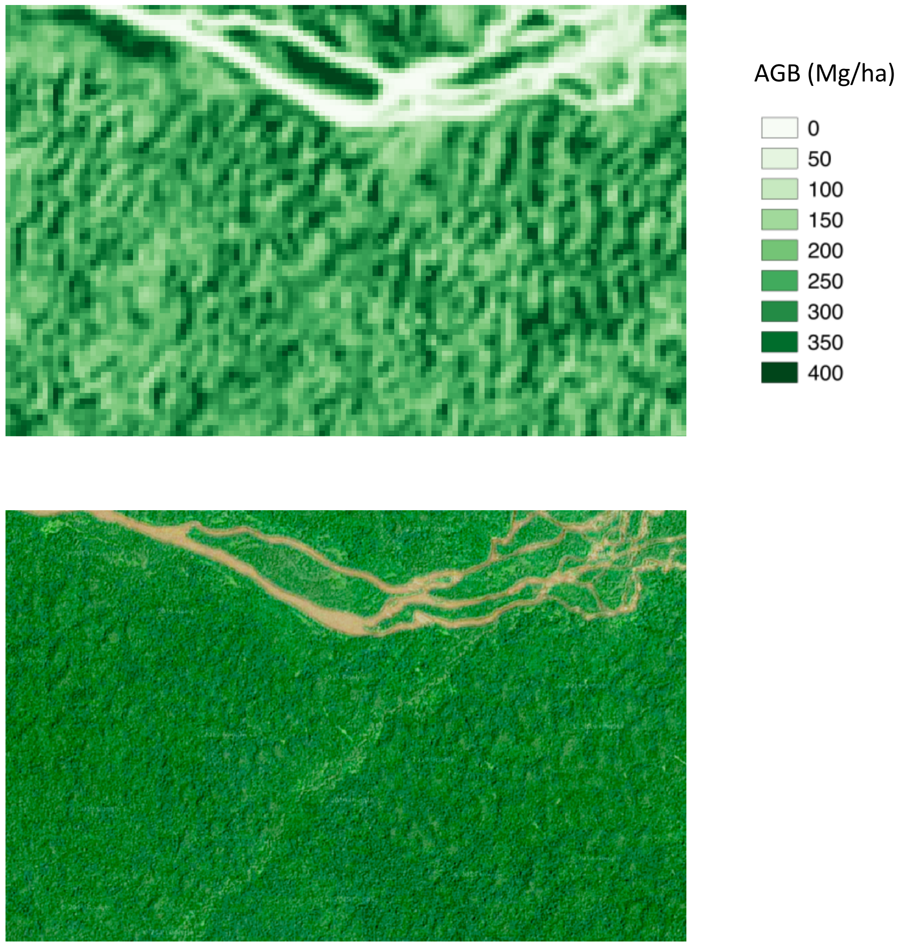

Figure 3-14: Example of topography-induced modulation of AGB estimates (top) and corresponding optical image from Google Earth to be considered as reference for the landscape (bottom). Uncompensated topography caused a variation of up to 200 Mg/ha between slopes facing the radar (light green areas) and slopes looking away from the radar (dark green areas).

Topography-induced distortions strongly decrease the level of confidence of the AGB estimates at the original spatial resolution of 1 hectare. By averaging over several adjacent pixels, the effect of topography reduces; however, the AGB level is somewhat lower than in reality, which needs to be accounted for when interpreting the averaged AGB maps.

3.4.4. Mangroves

The BIOMASAR algorithms rely on a simplified model (the Water Cloud Model) that describes the behaviour of the SAR backscatter as a function of biomass. The ability of this model to reproduce the relationship between SAR backscatter observations and biomass has been demonstrated in a large variety of forest types. However, when this functional dependence does not hold true, the model is not able to provide correct estimates of AGB. By checking against other datasets of forest variables (canopy height, biomass etc.), we identified a clear modelling issue in mangrove forests. Mangroves often exhibit a strong decrease of backscatter with increasing biomass [RD-5], which is the opposite of what the Water Cloud Model predicts. This causes strong underestimation of AGB in the CCI BIOMASS map displayed in Figure 3-15 when compared to an AGB product specifically tailored for mangroves and based on elevation data and allometries (Simard et al., 2019). The CCI BIOMASS dataset does not appear to follow the spatial distribution of the mangrove AGB map and often lies well below the AGB estimated in the latter. Although estimation of AGB from canopy height and regional height-to-biomass allometry appears to be more reliable than the solution implemented in CCI BIOMASS, the lack of a DEM for 2017 implied that the approach proposed by Simard et al. (2019) could not be implemented. Understanding, however, how signal changes in EO data can be related to the original map by Simard et al. could be a way to provide an updated estimate of AGB for mangroves that avoids such biases. The alternative would be to rely on different models to retrieve AGB specifically in mangrove forests.

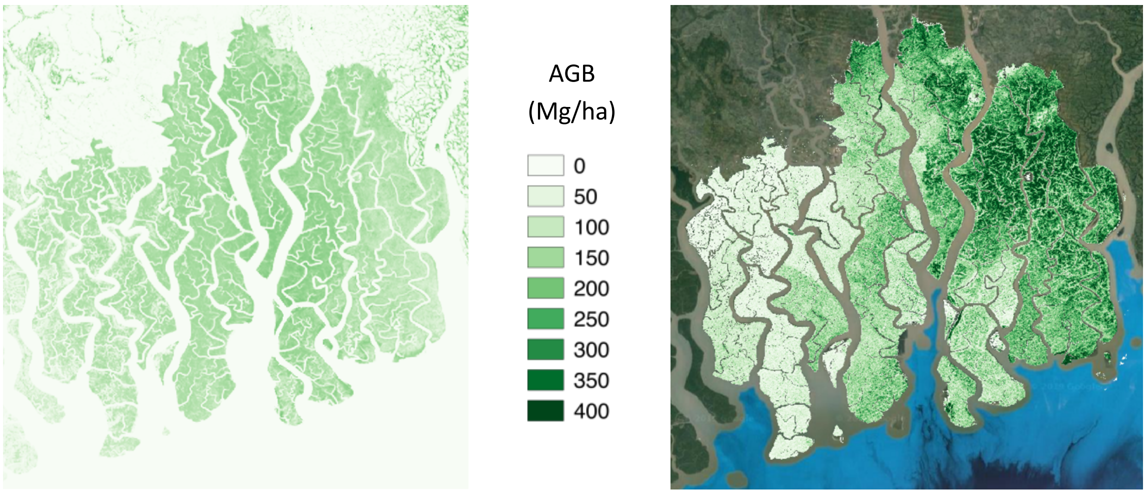

Figure 3-15: Estimates of AGB for mangrove forests of Bangladesh from the CCI BIOMASS dataset of 2017 (left) and the global mangrove AGB dataset for the year 2000 by Simard et al. (2019).

4. AGB change maps

To estimate AGB change, the Climate Research Data Package of the CCI Biomass suggests using 2018 as the reference year and taking the difference between (i) 2018 and 2010 and (ii) 2018 and 2017. Positive values represent a gain of AGB, negative values represent a loss of AGB. The precision of the AGB change estimates is defined as the square root of the sum of the variances of the two individual maps. Because of the different type of data available for each of the three epochs, a quality flag is provided. The quality flag expresses whether the AGB histograms associated with a pixel at the two epochs overlap or are disjoint.

Assuming that AGB1 and AGB2 are two estimates at epoch 1 and epoch 2, with epoch 1 prior to epoch 2. The follow scenarios can occur

- Significant difference (AGB2<<AGB1), i.e., disjoint histograms, corresponding to an AGB loss
- Potential loss (AGB2<AGB1) i.e., partially overlapping histograms
- Insignificant difference, i.e., overlapping histograms, corresponding to no change
- Potential gain (AGB2>AGB1) i.e., partially overlapping histograms
- Significant difference (AGB2>>AGB1), i.e., disjoint histograms, corresponding to an AGB gain

The AGB difference between two epochs is not provided as part of the CCI Biomass data package. Users interested in AGB changes between two epochs compute the difference by subtracting one map from the other. The CRDP provides the standard deviation of the AGB difference and the quality flag layer of the AGB change for 2018 vs. 2010 and 2018 vs. 2017.

The AGB change SD data layer has the same specification of the corresponding AGB SD layers.

The quality flag layer is stored in byte format and adopts the following legend

0: AGB=0 in both maps

1: AGB loss

2: Potential AGB loss

3: Improbable change

4: Potential AGB gain

5: AGB gain

With respect to class 3, a pixel is also labelled as improbable change when the conditions leading to a gain are satisfied but the difference is larger than the largest potential growth. For largest potential growth we assumed a value of 10 Mg ha^{-1} $year^{-1}$, which includes all types of natural forests and most plantations (IPCC, 2019).

It is strongly advised to use the quality flag map of the AGB change product when evaluating the AGB change data products (AGB difference and AGB difference standard deviation)! The AGB change products are prototypes, with large uncertainties.

Figure 4-1Figure 4-3 show a full resolution example of AGB and AGB change data products. The examples refer to a standard 10° x 10° tile as distributed by the CCI Biomass project, covering the region of Manaus, Brazil (extent of tile: Lat: 0°N, 10°S; Lon: 60°W, 50°W). In the following we illustrate the AGB dataset (for 2018 only), the AGB standard deviation (for 2018 only) and the AGB change products for 2018-2017 and 2018-2010.

The AGB dataset shows high AGB in undisturbed tropical forest and low values in areas affected by recent deforestation. The Amazon River crosses the image tile from West to East in the northern part of the tile. The image of the SD shows a fairly constant value of about 40% of the estimated value in intact forests. Higher values are observed in deforested regions. This is probably a consequence of higher uncertainty in the model parameters expressing the backscattering coefficient of the ground than in the model parameter expressing the backscattering coefficient of the vegetation.

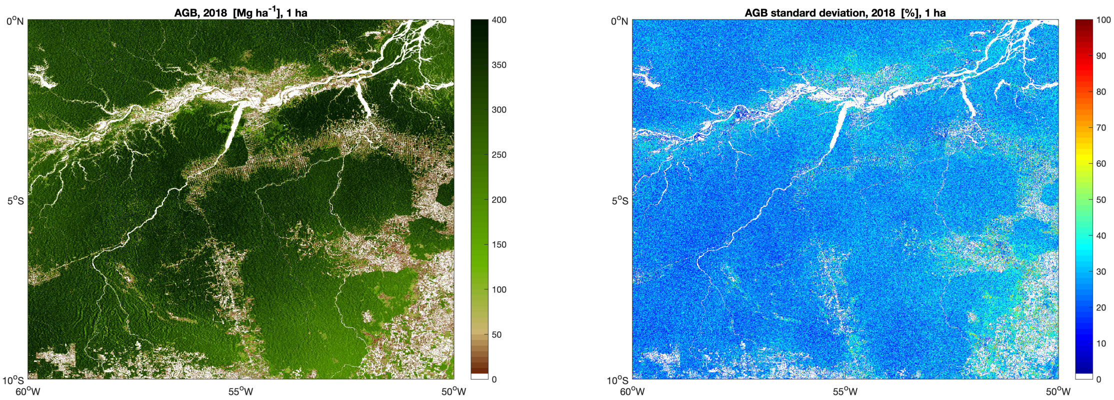

Figure 4-1: AGB (left) and AGB SD (right) for 2018. The colour ramps are constrained between 0 and 400 Mg ha-1 (AGB) and between 0% and 100% of the estimated AGB (AGB SD) to increase the colour contrast.

By taking the difference of the AGB maps of 2018 and 2017, we obtain the image illustrated in the left panel of Figure 4-2. There is a slight tendency towards positive values, which may either be attributed to growth or to different AGB estimation biases affecting each of the individual maps. The corresponding SD is shown in the right panel of Figure 4-2. The AGB of the change is higher than the AGB SDs because variances add. Since the overall SD is close to 100% of the estimated change, the SD layer already provides a clear indication on the reliability of the AGB changes. The quality flag in Figure 4-3 gives more direct evidence of the reliability of the AGB change map in Figure 4-2. Most pixels (practically all in intact forests) are labelled as improbable change, meaning that either the distribution of the AGB estimates at the two epochs strongly overlap or the difference is larger than the largest potential growth. AGB losses and gains are concentrated in areas affected by deforestation (Figure 4-3).

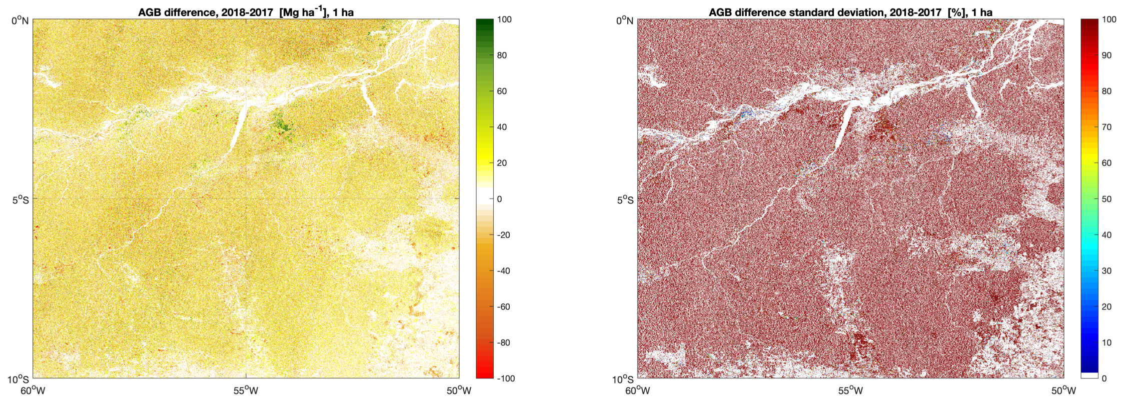

Figure 4-2: AGB change (left) and corresponding SD (right) between 2017 and 2018. AGB change is defined as difference between AGB maps of 2018 and 2017. The colour ramps are constrained between -/+100 Mg ha-1 (AGB change) and between 0% and 100% (AGB change SD) to increase the colour contrast.

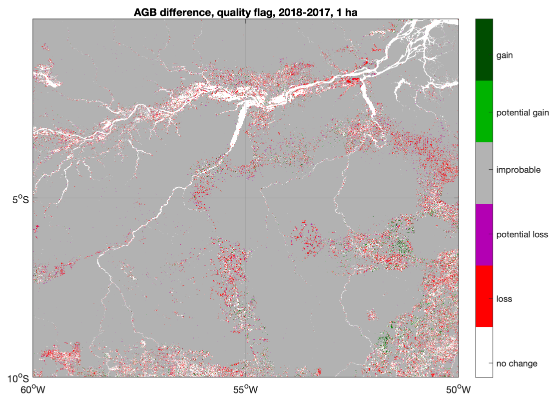

Figure 4-3: Quality flag of AGB change between 2017 and 2018.

The relevance of the quality flag becomes clearer when interpreting the AGB changes between 2010 and 2018 (Figure 4-4). Because of the different EO datasets, the difference, even in intact forests, is large and corresponds to a decrease of AGB between 2010 and 2018, which is highly improbable. The largest differences occur at the edges of forests affected by deforestation, which is more realistic. The AGB change SD (Figure 4-4) is large but in principle not too large to be able to interpret the AGB change correctly. The quality flag (Figure 4-5) provides clear indications that most of the changes are improbable, because the difference was larger than the maximum increment allowed by growth. The quality flag indicates that AGB losses and gains occur in areas of ongoing deforestation. A gain of AGB in these areas is often associated with an increase of AGB from 0 to a very low biomass.

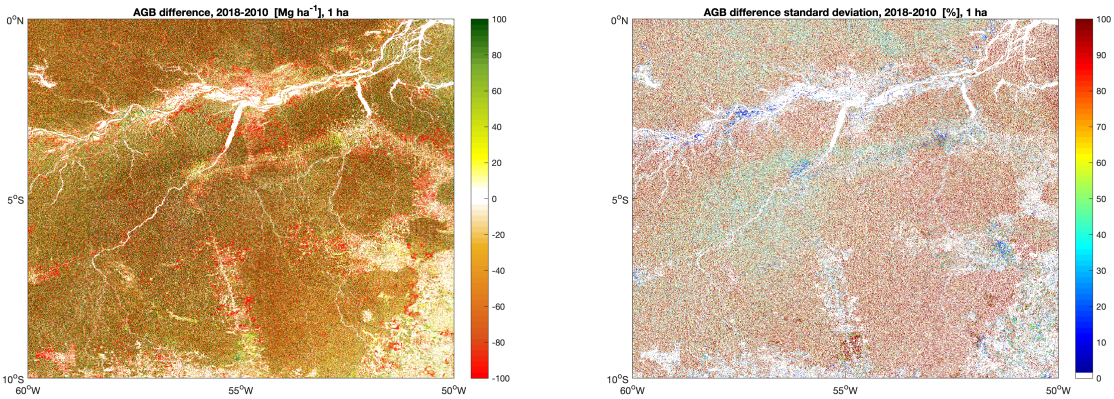

Figure 4-4: AGB change (left) and corresponding SD (right) between 2010 and 2018. AGB change is defined as difference between AGB maps of 2018 and 2010. The colour ramps are constrained between -/+100 Mg ha-1 (AGB change) and between 0% and 100% (AGB change SD) to increase the colour contrast.

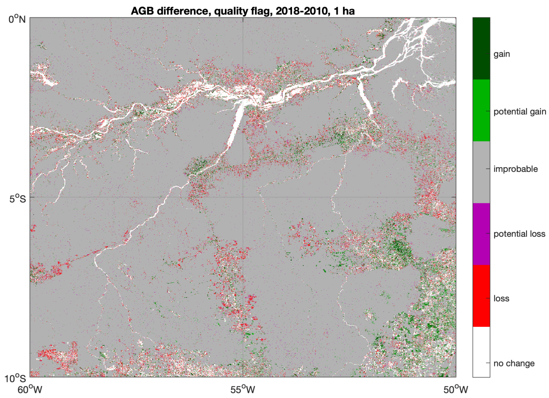

Figure 4-5: Quality flag of AGB change between 2010 and 2018.

4.1 Assessing AGB changes with a bias correction

Errors and uncertainties affecting the individual maps suggest a very careful approach to the AGB change maps and discourage the use of individual pixels. The quality flag layer is a fundamental instrument to guide users on how to use the AGB change maps. The evidence that the AGB maps are affected by different biases suggests: (i) estimation of the epoch-specific biases and (ii) assessment of AGB changes with and without a bias correction.

We try to model the bias as a function of AGB (mapped) as well as other spatially exhaustive covariates (Table 4-1) using a Random Forest model (for details, see [RD-3]). The bias models are cross-validated (10-fold) and assessed through Root Mean Square Error (RMSE), Mean Absolute Error (MAE) and R^2. The predictive power of the covariates is evaluated using variable importance measures while sensitivity of the modelled trends to its inputs is assessed using partial dependence plots. If fitting the bias trend model is successful, the RF model is used in predictive mode to predict a global bias layer.

Table 4-1: Bias models.

CCI map epoch	Bias predictors	Cross-validation results	Remarks
2010	AGB map, SD layer, Tree Cover 2010, slope, aspect, biome, Intact Forest Landscapes 2010	R^2 = 0.35 RMSE= 18.31 Mg/ha MAE= 13.24 Mg/ha	Excluded plots >7 years older to be more consistent with the training data among periods
2017	AGB map, SD layer, Tree Cover 2015, slope, aspect, biome, Intact Forest Landscapes 2015	R^2 = 0.38 RMSE=18.38 Mg/ha MAE=13.98 Mg/ha	
2018	AGB map, SD layer, Tree Cover 2015, slope, aspect, biome, Intact Forest Landscapes 2015	R^2 = 0.34 RMSE=19.10 Mg/ha MAE=14.49 Mg/ha	

For each epoch, a bias layer with a pixel size of 0.1° was created.

Figure 4-6Figure 4-7 show the bias layers for the years 2010 and 2018. In 2010, the bias layer indicates that the AGB was underestimated except for the Eurasian boreal zone where apparently the AGB was slightly overestimated (Figure 4-6). The bias layer for 2018 shows somewhat different patterns (Figure 4-7), with slight overestimation in intact tropical forests and slightly less overestimation in boreal zones. These results indicate that a global assessment of AGB changes would need to account for the different biases affecting the CCI maps in order to avoid wrong conclusions about the location and the magnitude of carbon sinks and sources.

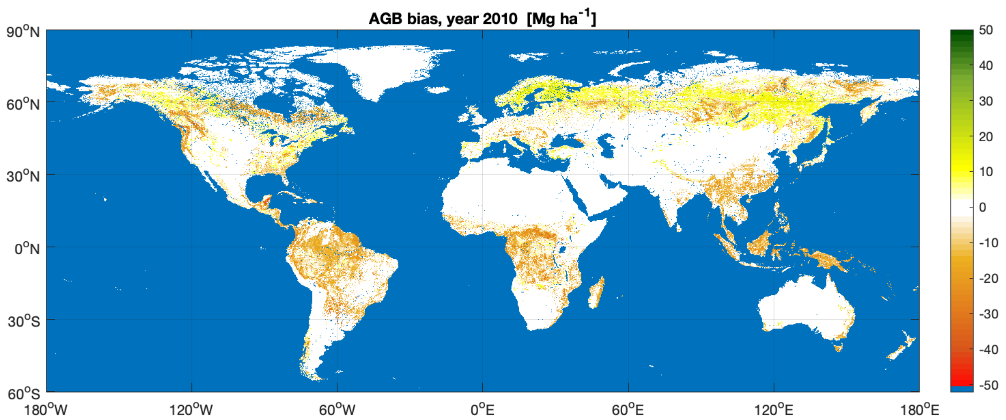

Figure 4-6: Estimated bias for the AGB map of 2010. Pixel size 0.1°.

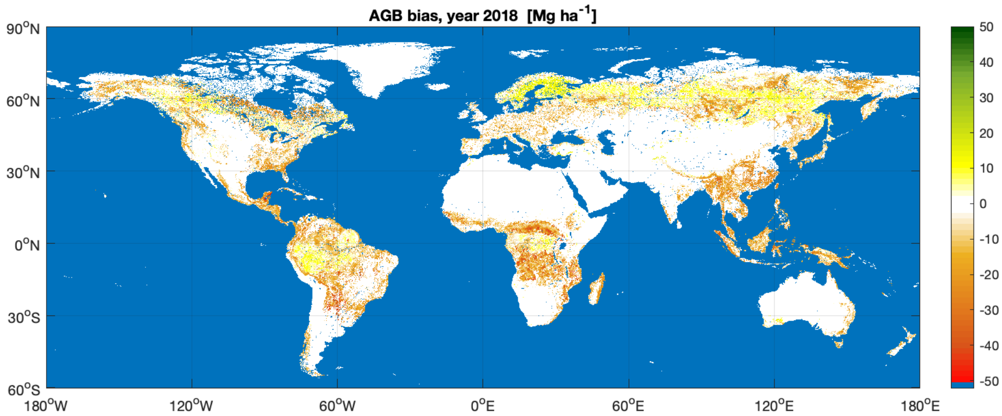

Figure 4-7: Estimated bias for the AGB map of 2018. Pixel size 0.1°.

Working at 0.1° spatial scale, Figure 4-8 and Figure 4-9 show the AGB change maps for 2018 vs. 2010 without and with bias correction [RD-3]. Between 2010 and 2018, AGB changes due to growth, forest cover loss etc. can be expected. Several large-scale increases shown in Figure 4-8 have unrealistic magnitude (e.g., Amazon, Canadian taiga, Insular Southeast Asia). We attribute such errors to the different composition of the remote sensing dataset in 2010 (a single ALOS PALSAR observation and co-polarized C-band ASAR data) and 2018 (multi-temporal ALOS-2 PALSAR-2 observations in the tropics, more inhomogeneity in the ALOS-2 mosaic and dual-polarized Sentinel-1 data). Bias correction reduced the magnitude of the AGB increase in the tropics (Figure 4-9). In the boreal zone, the AGB difference increased after bias correction (Figure 4-9). While the correction for biases appears to provide a plausible estimate of the AGB changes between 2010 and 2018, being consistent with other evidence (greening of the northern latitudes, increased productivity of southern temperate forests, reduced carbon sink in the tropics), there is a need for a quantitative assessment to confirm the validity of the results.

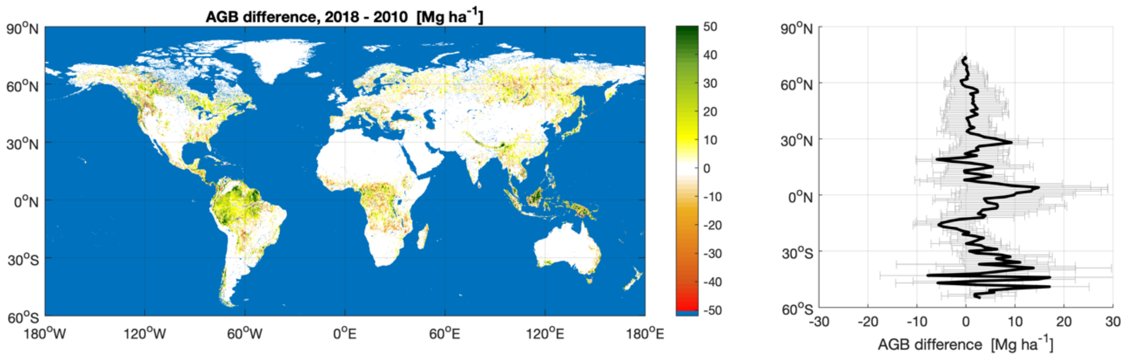

Figure 4-8: AGB change between 2010 and 2018 (left) and latitudinal average of AGB changes (right).

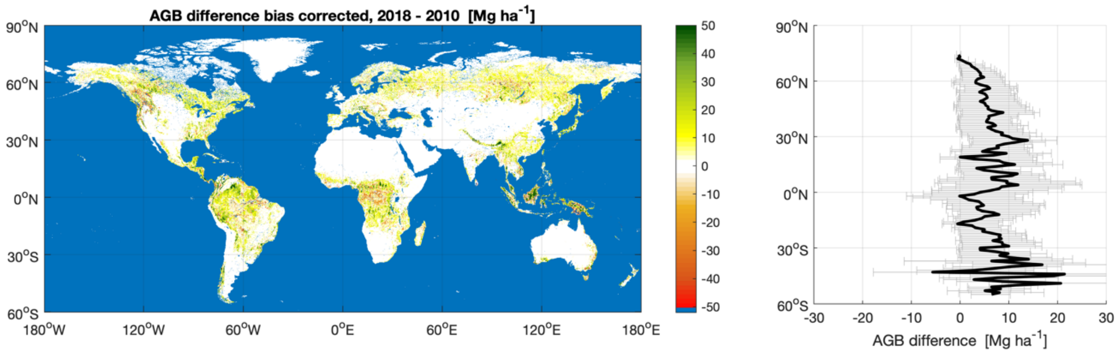

Figure 4-9: AGB change between 2010 and 2018 after bias correction (left) and latitudinal average of bias-corrected AGB changes (right).

Bias layers and bias-corrected datasets (0.1° pixel size only) can be obtained on demand.

5. Usage notes

As a result of our investigation of the three AGB datasets and related changes, users are kindly invited to note the following comments:

- Use of the AGB estimates of individual full resolution pixels should be avoided.
- The 2018 AGB dataset has (locally) higher quality than the 2017 AGB dataset
- The 2010 CCI BIOMASS dataset is an improved version of the GlobBiomass AGB dataset (http://globbiomass.org) but has different properties compared to 2017 and 2018.
- AGB change maps should be interpreted carefully. It is strongly advised to use the quality flag layer to understand the reliability of the AGB change values.
- Be extremely cautious when using the CCI Biomass maps to assess AGB changes. We strongly advice to validate changes before further analysis of the data.

6.Data access and policy

The CCI BIOMASS products are made available through the CCI data portal (https://climate.esa.int/en/odp/#/project).

With the most recent version of the CRDP, the following data products are available

- AGB maps for the years 2010, 2017 and 2018, including per-pixel SD, version 3.0;
- AGB change maps for the years 2018-2017 and 2018-2010 can be computed from the AGB maps. Per-pixel SD and quality flags, QF, version 3.0, are available on the data portal.

The CCI BIOMASS datasets have been processed by the CCI BIOMASS consortium led by the University of Aberystwyth (U.K.). They are made available to the public by ESA and the consortium. You may use one or several CCI BIOMASS products for educational and/or scientific purposes, without any fee on the condition that you credit the ESA Climate Change Initiative and in particular its BIOMASS project as the source of the data:

Copyright notice: © ESA Climate Change Initiative - BIOMASS project 2021.

Any scientific publication on the results of research activities based on CCI BIOMASS data products should acknowledge the ESA CCI BIOMASS project in the text of the publication and provide the project with an electronic copy of the publication (see https://climate.esa.int/en/projects/biomass/ for contacts).

If CCI BIOMASS data products are to be used in advertising or commercial promotion, the ESA CCI BIOMASS project should be acknowledged and the layout should be submitted to the project for approval beforehand (see https://climate.esa.int/en/projects/biomass/ for contacts).

7. References

Buchhorn, M.; Smets, B.; Bertels, L.; Lesiv, M.; Tsendbazar, N.-E.; Herold, M.; Fritz, S.; Copernicus Global Land Service: Land Cover 100m: Collection 2: epoch 2015. Dataset of the global component of the Copernicus Land Monitoring Service. DOI 10.5281/zenodo.3243509 (in prep)

Committee on Earth Observation Satellites, 2008, Working Group on Information Systems and Services - Interoperability Handbook, February 2008 Issue 1.1. Available at: http://www.eohandbook.com/

ESA Climate Office, CCI Data Standards, CCI-PRGM-EOPS-TN-13-0009, version 2.1, date 02/08/2019

Ferraz, A., Saatchi, S., Xu, L., Hagen, S., Chave, J., Yu, Y., Meyer, V., Garcia, M., Silva, C., Roswintiart, O., Samboko, A., Sist, P., Walker, S., Pearson, T.R.H., Wijaya, A., Sullivan, F.B., Rutishauser, E., Hoekman, D., Ganguly, S., 2018. Carbon storage potential in degraded forests of Kalimantan, Indonesia. Environ. Res. Lett. 13, 095001. https://doi.org/10.1088/1748-9326/aad782

Hajnsek, I., Pardini, M., Jäger, M., Horn, R., Kim, J.S., Jörg, H., Papathanassiou, K., Dubois-Fernandez, P., Dupuis, X., Wasik, V., 2017. Technical Assistance for the Development of Airborne SAR and Geophysical Measurements During the AFRISAR Experiment. Final Report, Deliverable DD-4. pp. 152.

IPCC Good Practice Guidance for Land Use, Land-Use Change and Forestry, Penman, J., Gytarsky, M., Hiraishi, T. et al., Intergovernmental Panel on Climate Change, 2003, ISBN 4-88788-003-0, available at http://www.ipccnggip.iges.or.jp/public/gpglulucf/gpglulucf_contents.html

IPCC, 2019. 2019 Refinement to the 2006 IPCC Guidelines for National Greenhouse Gas Inventories. Volume 4: Agriculture, Forestry and Other Land Use.

Longo, M., Keller, M., dos-Santos, M.N., Leitold, V., Pinagé, E.R., Baccini, A., Saatchi, S., Nogueira, E.M., Batistella, M., Morton, D.C., 2016. Aboveground biomass variability across intact and degraded forests in the Brazilian Amazon: AMAZON INTACT AND DEGRADED FOREST BIOMASS. Global Biogeochem. Cycles 30, 1639–1660. https://doi.org/10.1002/2016GB005465

Ploton, P., Mortier, F., Barbier, N., Cornu, G., Réjou-Méchain, M., Rossi, V., Alonso, A., Bastin, J.-F., Bayol, N., Bénédet, F., Bissiengou, P., Chuyong, G., Demarquez, B., Doucet, J.-L., Droissart, V., Kamdem, N.G., Kenfack, D., Memiaghe, H., Moses, L., Sonké, B., Texier, N., Thomas, D., Zebaze, D., Pélissier, R., Gourlet-Fleury, S., 2020. A map of African humid tropical forest aboveground biomass derived from management inventories. Scientific Data 7:221, 13. https://doi.org/10.1038/s41597-020-0561-0

Rosenqvist, A., Shimada, M., Ito, N., Watanabe, M., 2007. ALOS PALSAR: A pathfinder mission for global-scale monitoring of the environment. IEEE Trans. Geosc. Rem. Sens. Vol. 45, 3307–3316. https://doi.org/10.1109/TGRS.2007.901027

Santoro, M., Cartus, O., Carvalhais, N., Rozendaal, D., Avitabilie, V., Araza, A., de Bruin, S., Herold, M., Quegan, S., Rodríguez Veiga, P., Balzter, H., Carreiras, J., Schepaschenko, D., Korets, M., Shimada, M., Itoh, T., Moreno Martínez, Á., Cavlovic, J., Cazzolla Gatti, R., da Conceição Bispo, P., Dewnath, N., Labrière, N., Liang, J., Lindsell, J., Mitchard, E.T.A., Morel, A., Pacheco Pascagaza, A.M., Ryan, C.M., Slik, F., Vaglio Laurin, G., Verbeeck, H., Wijaya, A., Willcock, S., 2020. The global forest above-ground biomass pool for 2010 estimated from high-resolution satellite observations (preprint). Earth System Science Data Discussions, https://doi.org/10.5194/essd-2020-148.

Shimada, M., 2010. Ortho-rectification and slope correction of SAR data Using DEM and its accuracy evaluation. IEEE Journal of Selected Topics in Applied Earth Observations and Remote Sensing, 3 (4), 657-671.

Shimada, M. and Ohtaki, T., 2010. Generating large-scale high-quality SAR mosaic datasets: Application to PALSAR data for global monitoring. IEEE Journal of Selected Topics in Applied Earth Observations and Remote Sensing, 3 (4), 637-656.

Simard, M., Fatoyinbo, L., Smetanka, C., Rivera-Monroy, V.H., Castaneda-Moya, E., Thomas, N., Van der Stocken, T., 2019. Mangrove canopy height globally related to precipitation, temperature and cyclone frequency. Nature Geoscience 12, 40–45.

Ulander, L.M.H., Gustavsson, A., Flood, B., Murdin, D., Dubois-Fernandez, P., Dupuis, X., Sandberg, G., Soja, M.J., Eriksson, L.E.B., Fransson, J.E.S., Holmgren, J., Wallerman, J., 2011. BioSAR 2010 - Technical assistance for the development of airborne SAR and geophysical measurements during the BioSAR 2010 experiment.

8. Appendicies

8.1 Appendix A – NetCDF attributes

The description of the CCI Biomass global aboveground biomass (AGB) products is based on the structure of the NetCDF files. The global attributes of the biomass map are described in Table A1.

Table A1: Global attributes of the global AGB map delivered by the CCI Biomass project, following the structure of the NetCDF files.

Attribute Name	Format	Value	Description
Title		ESA CCI above-ground biomass product level 4, year 2010, 2017 or 2018	Product identifier
Institution		Gamma Remote Sensing	Where the data has been produced

Source		ALOS-2 PALSAR-2 FB and WB mosaics, Sentinel-1 GRD	Source of the original data
History		GSV estimation with BIOMASAR-L, v201906 GSV estimation with BIOMASAR-C, v201906 Merging of GSV estimates, v201906 Conversion of GSV to AGB, v201711	List of applications that have modified the ALOS-2 PALSAR-2, Sentinel-1 data, with time stamp, processor and parameters
references		http://cci.esa.int/biomass	References that describe the data or methods used to produce it.
tracking_id		4e618436-c170-3165-8781-046b3aff5bf3	UUID, Universal Unique Identifier
Conventions		CF-1.7	Name of the conventions followed
product_version		1.0	Version of AGB product
summary		This dataset contains a global map of above-ground biomass of the epoch 2017 obtained from L-and C-band spaceborne SAR backscatter, placed onto a regular grid.	
keywords		satellite, observation, forest, biomass	
id		ESACCI-BIOMASS-L4-AGB-MERGED-100m-2017-fv1.0.nc	Product identifier
naming authority		ch.gamma-rs	
keywords vocabulary		NASA Global Change Master Directory (GCMD) Science Keywords	
cdm_data_type		INT	
comment		These data were produced at ESA CCI as part of the ESA Biomass CCI project.	Miscellaneous information about the data or method used to produce it
date_created	yyyy-MM-dd'T'HH:mm:ss'Z'	20190708T000000Z	Creation time of product

creator_name		Gamma Remote Sensing	
creator_url		http://www.gamma-rs.ch	
creator_email		santoro@gamma-rs.ch	
project		Climate Change Initiative - European Space Agency	
geospatial_lat_min	-90.0 ... 90.0	-60	South border of the bounding box
geospatial_lat_max	-90.0 ... 90.0	80	North border of the bounding box
geospatial_lon_min	-180.0 ... 180.0	-180	West border of the bounding box
geospatial_lon_max	-180.0 ... 180.0	180	East border of the bounding box
geospatial_vertical_min		0	
geospatial_vertical_max		0	
time_coverage_start		20170101T000000Z	
time_coverage_end		20171231T235959Z	
time_coverage_duration		P1Y	
time_coverage_resolution		P1Y	
standard_name_vocabulary		NetCDF Climate and Forecast (CF) Metadata Convention version 67	
license		ESA CCI Data Policy: free and open access	
platform		ALOS-2, Sentinel-1A, Sentinel-1B	
sensor		PALSAR-2, SAR-C	
spatial_resolution		100 m	
geospatial_lat_units		degrees_north	
geospatial_lon_units		degrees_east	
geospatial_lon_resolution		0.000888888	
geospatial_lat_resolution		0.000888888	
key_variables		agb	
format_version		CCI Data Standards v2.1	

The variables and variables' attributes of the global AGB NetCDF file are presented in Table A2.

Table A2. Variables and variables' attributes of the global AGB map delivered by the CCI BIOMASS project, following the structure of the NetCDF files.

Variable	Attribute	Format	Value	Description
crs		int		Coordinate reference system attribute container
	grid_mapping_name		Latitude-Longitude	
	semi_major_axis		6378137.0	
	inverse_flattening		298.257223563	
	false_easting		0.0	
	false_northing		0.0	
	longitude_of_central_meridian		0.0	
	scale_factor_at_central_meridian		1.0	
time		double(time)		Start time of the multi-year period
	standard_name		time	
	long_name		single-year period	
	units		time since reference time	days since 1990-1-1 0:0:0
lon		double (lon)	-180.0 .. 180.0	Longitude coordinate of image column
	standard_name		Longitude	
	long_name		WGS84 longitude coordinate	
	units		degrees east	
	valid_min		-180.0	
	valid_max		180.0	
lat		double (lat)	-60.0 .. 80.0	Latitude coordinate of image row
	standard_name		latitude	
	long_name		WGS84 latitude coordinate	
	units		degrees north	
	valid_min		-60.0	
	valid_max		80.0	

agb		int16 (lat,lon)		AGB value
	standard_name		n/a	
	long_name		Above-ground biomass	
	valid_min		0	
	valid_max		10000	
	_FillValue		99999	
agb_se		int16 (lat,lon)		Standard deviation of AGB value
	standard_name		n/a	
	long_name		Above-ground biomass standard deviation	
	valid_min		0	
	valid_max		65536	
	_FillValue		99999	